Ichnos, 21:158–174, 2014

ISSN: 1042-0940 print / 1563-5236 online
DOI: 10.1080/10420940.2014.930036

Taylor & Francis
Taylor & Francis Group

Sabkha and Burrow-Mediated Dolomitization in the Mississippian Debolt Formation, Northwestern Alberta, Canada

Greg M. Baniak, Larry Amskold, Kurt O. Konhauser, Karlis Muehlenbachs, S. George Pemberton, and Murray K. Gingras

Department of Earth and Atmospheric Sciences, University of Alberta, Edmonton, Alberta, Canada

Dolomitized burrows in the Mississippian (Visean) Debolt Formation of northwestern Alberta, Canada form the primary reservoir intervals in the Dunvegan gas field. Sedimentological and ichnological analyses suggest a carbonate ramp setting that includes subenvironments such as sabkhas, hypersaline lagoons, restricted subtidal lagoons, intertidal mud flats, and peloidal shoals. Dolomitization occurs primarily within oxidized muds and highly bioturbated sediments, with the primary mode being sabkha-associated precipitation. In this context, dolomitization within the burrows also appears to be mediated by sulfate-reducing bacteria. δ^{18}O values for dolomite within burrows (mean 2.4‰) are enriched by 1.3‰ relative to calcite values (mean 1.1‰) within the burrows. This degree of fractionation is similar for dolomite and calcite that have precipitated from the same solution. It is therefore suggested that the protodolomite precipitated in equilibrium with calcite rather than by replacement of pre-existing calcite. Isotopic values of δ^{13}C measured for dolomite associated with burrows (mean 3.4‰) and matrix (mean 3.5‰) is slightly enriched relative to measured calcite values (mean 3.2‰ for matrix; mean 3.1‰ for burrows). These isotopic trends are common for modern dolomite that has precipitated in equilibrium with seawater where concomitant sulfate reduction and organic carbon-oxidation is inferred to occur near the surface.

Keywords Ichnology, Facies, Isotopes, Burrow-associated dolomite, Sabkha, Bacterial sulfate reduction

INTRODUCTION

The study of dolomite has a long and extensive history, dating back to the pioneering work of Giovanni Arduino and Déodat Gratet de Dolomieu in the 18th century. Despite being an abundant mineral in the rock record, dolomite distribution is limited in modern sedimentary environments. Kinetic energy barriers such as high hydration energies of the magnesium ion (Mg^{2+}) (Markham et al., 2002), low concentration and activities of the carbonate ion (CO_3^{2-}), and the presence of sulfate ions (Morrow, 1982; Budd, 1997) are all major inhibiting factors in abiotic dolomite precipitation. Despite this knowledge, replicating dolomite precipitation under modern physico-chemical conditions in the laboratory has proven futile (McKenzie, 1991; Land, 1998). The formation of dolomite and the nature of the dolomitizing fluids remains controversial and is widely referred to as the "dolomite problem" (Gunatilaka, 1987; Arvidson and Mackenzie, 1999; Machel, 2004). Classic models such as evaporative pumping, hydrothermal circulation, seepage reflux, sabkha, seawater convection, burial diagenesis, and subsurface mixing have been invoked to explain dolomitization within the rock record (Hsü and Siegenthaler, 1969; Morrow, 1982; Machel and Mountjoy, 1986; Warren, 2000; Machel, 2004).

In this context, burrow-associated diagenesis has recently emerged as another model for shallow-burial dolomitization. This is due to textural and compositional heterogeneities (e.g., concentration of extracellular polysaccharides in burrow walls and contrasts in permeability) associated with biogenic sedimentary structures (Gingras et al., 2004; Rameil, 2008; Corlett and Jones, 2012). Although occurrences of dolomitized burrows within the rock record are common (e.g., Baniak et al., 2013; Beales, 1953; Kendall 1977a; Morrow, 1978; Zenger, 1996; Keswani, 1999), the timing and cause of dolomitization associated with the burrows can be difficult to determine.

Within modern environments, microbial sulfate reduction (MSR) plays an integral role in the precipitation of dolomite at near-surface temperatures (Vasconcelos et al., 1995;

Address correspondence to Greg M. Baniak, Department of Earth and Atmospheric Sciences, 1-26 Earth Sciences Building, University of Alberta, Edmonton, Alberta, Canada, T6G 2E3. E-mail: baniak@ualberta.ca.

Greg M. Baniak's current affiliation is BP Canada Energy Group ULC, Calgary, Alberta, Canada. Larry Amskold's current affiliation is Jacobs Engineering, 4300 B Street, Suite 600 Anchorage, AK 99503, USA.

Color versions of one or more of the figures in the article can be found online at www.tandfonline.com/gich.

Warthmann et al., 2000; van Lith et al., 2003; Krause et al., 2012). Examples include the hypersaline lagoons of Lagoa Vermelha and Brejo do Espinho, northeastern coast of Brazil (Vasconcelos et al., 1995, 2005; Vasconcelos and Mackenzie, 1997; Warthmann et al., 2005) and the ephemeral lakes of the Coorong Region of South Australia (Von der Borch and Lock, 1979; Wright and Wacey, 2005; Wacey et al., 2007). Such studies are invaluable as they help outline the manner in which microbes influence the physiochemical parameters that can help mediate early dolomitization within modern sediments.

The focus of this study is the Mississippian (Visean) Debolt Formation located in the Dunvegan gas field of northwestern Alberta (Fig. 1). Located at depths greater than 1400 m, the Dunvegan gas field has reserves within a 3.4×10^{10} m^3 to 4.5×10^{10} m^3 (1.2 to 1.6 trillion cubic feet) range (Al-Aasm and Packard, 2000; Packard et al., 2004). These reserves make the Dunvegan gas field the second largest carbonate-hosted non-reefal gas field in the Western Canadian Sedimentary Basin (Al-Aasm and Packard, 2000). Reservoir production occurs primarily from highly porous microsucrosic dolomites occurring within the bioturbated fabrics (Packard et al., 2004). The preferred dolomitization of the burrow fabrics suggests certain parameters (e.g., the presence of MSR, low oxygenation, high salinity) must have existed. The purpose of this article is to document the lithofacies and their paleogeographic distribution within the Dunvegan gas field. From this, an understanding of the environmental settings that helped mediate dolomitization within the burrows will be analyzed by integrating lithologic, petrographic, and isotopic analysis.

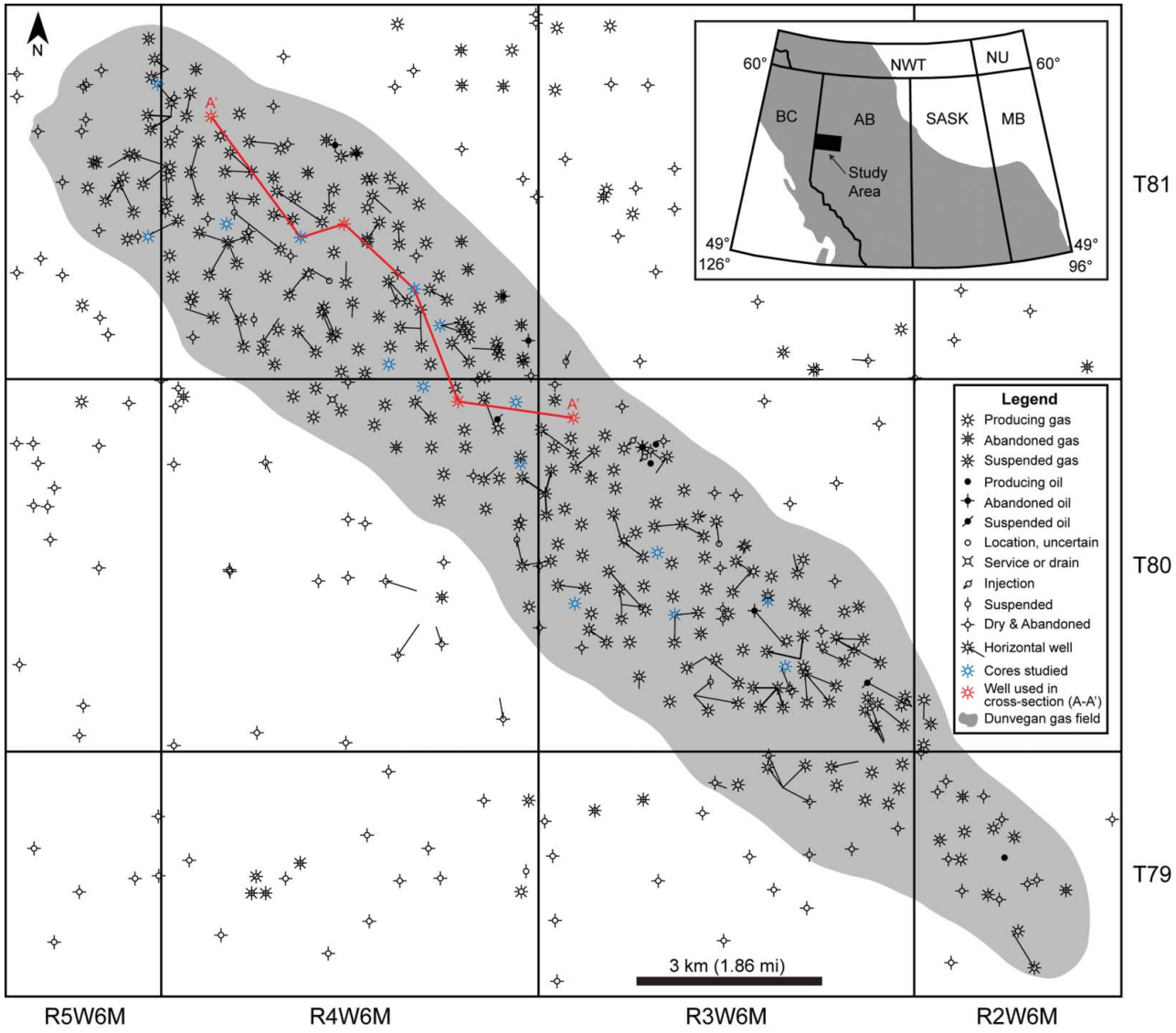

FIG. 1. Location map of the Dunvegan gas field in northwestern Alberta that produces from the Mississippian (Visean) Debolt Formation. In the study area, 15 cored wells (demarcated in blue) were studied. The wells used in the cross-section (A-A', Fig. 4) are demarcated in red. (See Color Plate I.)

IMPACT OF BIOTURBATION ON SUBSTRATE BIOGEOCHEMISTRY

Infaunal invertebrates, such as crustaceans, insects, and earthworms, commonly modify sediment through particle remobilization and grazing (Aller, 1994; Bromley, 1996; Gingras et al., 2007a). A common by-product of bioturbation is the introduction of labile organic matter, such as mucous secretions and fecal material, into the substrate (Steward et al., 1996; Hauck et al., 2008; Pak et al., 2010). Mucous secretions, for instance, represent ideal microenvironments for microbes since many of the burrows are lined with organic materials such as extracellular polysaccharides (i.e., microbial exopolymer secretions) and glycoprotein mucin (Konhauser and Gingras, 2007, 2011; Lalonde et al., 2010; Petrash et al., 2011). For example, Gunnarsson et al. (1999a) observed that elevated concentrations of a tetrachlorobiphenyl commonly occurred in the thin mucous layer covering the burrow linings of the polychaete *Neries diversicolor* compared to the surrounding bulk sediment. Similar observations were also made by Gunnarsson et al. (1999b) for the linings of disk chamber and arm burrows of the brittle star *Amphiura filiformis*. These microbial exopolymer secretions (EPS) are important, as they are able to bind organic compounds of both high and low molecular weight (Decho, 1990). As a result, EPS comprises a significant portion of organic carbon within sediment (Confer and Logan, 1998) and acts as a reactive interface for the sorption of dissolved matter and secondary mineral precipitation (Mayer et al., 1999; Gunnarsson et al., 1999a, 1999b; Konhauser and Gingras, 2007, 2011).

The eventual decomposition of EPS and other organic material within bioturbated environments is critical in driving sedimentary metabolic reactions. In short, any organic carbon present usually becomes paired to a sequence of terminal electron accepting processes, with the more energetically favored reactions proceeding first (Froelich et al., 1979; Canfield et al., 1993; Chapelle et al., 1995). As a result of the decomposition of EPS, idealized biogeochemical reactions within sediments (e.g., Freolich et al., 1979) can become disrupted through activities such as bioturbation (Aller, 1982; Kristensen, 2000; Needham et al., 2004). In any event, these geochemical reactions are commonly microbially mediated and include (after Froelich et al., 1979 and Konhauser, 2007):

[1] Aerobic respiration:
CH_2O (organic carbon) + $O_2 \rightarrow CO_2 + H_2O$
[2] Nitrate reduction:
$2CH_2O + NO_3^- + 2H^+ \rightarrow 2CO_2 + NH_4^+ + H_2O$
[3] Mn(IV)-oxide reductive dissolution:
$CH_2O + 2MnO_{2(s)} + 4H^+ \rightarrow CO_2 + 2Mn^{2+} + 3H_2O$
[4] Fe(III)-oxyhydroxide reductive dissolution:
$CH_2O + 4FeOOH_{(s)} + 8H^+ \rightarrow CO_2 + 4Fe^{2+} + 7H_2O$
[5] Sulfate reduction:
$2CH_2O + SO_4^{2-} + H^+ \rightarrow HS^- + 2CO_2 + 2H_2O$
[6] Methanogenesis:
$2CH_2O \rightarrow CH_4 + CO_2$

Notably, the oxidation (or mineralization) of organic carbon leads to an increase in alkalinity (represented as CO_2) and an increase in pH (reactions 2 through 5). Studies of pore waters in deep-sea sediments (e.g., Froelich et al., 1979) and anoxic basins (e.g., Reeburgh, 1980) have shown that the most energetically favorable redox reactions occur first and concentrations of electron acceptors such as O_2 and NO_3 are typically the first to become depleted. Sulfate reduction (reaction 5) and methanogenesis (reaction 6) are therefore later-stage redox reactions. Consequently, high concentrations of organic carbon are required to consume these earlier terminal electron acceptors before the onset of the later reactions can occur. Notably, the contemporaneous bacterial mineralization of organic carbon and increase in pH will also help favor the formation of a carbonate ion due to the hydration of CO_2 to carbonic acid (H_2CO_3) and subsequent deprotonation reactions (i.e., $H_2CO_3 \rightarrow HCO_3^- + H^+ \rightarrow CO_3^{2-} + 2H^+$).

Modern studies by Garrison and Luternauer (1971) and Gunatilaka et al. (1987) have shown that organic material present within animal burrows helps promote the precipitation of dolomite. Given the ubiquitous presence of organic material within most burrows environments, development of a reducing microenvironment can occur (Gingras et al., 2004). Within reducing sediment, sulfate-reducing bacteria are present and are able to remove dolomite-inhibiting sulfate anions. As a result, liberation of the Mg^{2+} cation from the SO_4^{2-}-Mg^{2+} ion pair occurs, thereby increasing the availability of the free Mg^{2+} cations for early dolomite precipitation (van Lith et al., 2003). Elevated concentrations of sulfide have been measured in modern burrows (Waslenchuk et al., 1983), suggesting that sulfate reduction is indeed occurring within or adjacent to burrow systems.

REGIONAL GEOLOGICAL SETTING OF THE DEBOLT FORMATION

During the Mississippian and Pennsylvanian Periods in western Canada, the principal tectonic features were (i) Prophet Trough, (ii) Peace River Embayment, (iii) cratonic platform, (iv) Williston Basin, and (v) Yukon Fold Belt (Richards, 1989). The Debolt Formation and its stratigraphic equivalents are deposited primarily within the Prophet Trough and Peace River Embayment in British Columbia and Alberta (Fig. 2). The Prophet Trough is a downfaulted margin (i.e., distal foreland basin) that extends from the northern Yukon and Alaska southward to join the Antler Foreland Basin of the western United States (Richards, 1989; Richards et al., 1993, 1994). The Peace River Embayment (Douglas et al., 1970) can trace its origins to the structural evolution of the Peace River Arch (Cant, 1988; O'Connell et al., 1990). The Peace River Arch was a prominent east-northeast trending topographic high of Precambrian granites that were approximately 800–1,000 m above the regional elevation near the Alberta-British Columbia border during the early Paleozoic (Cant, 1988).

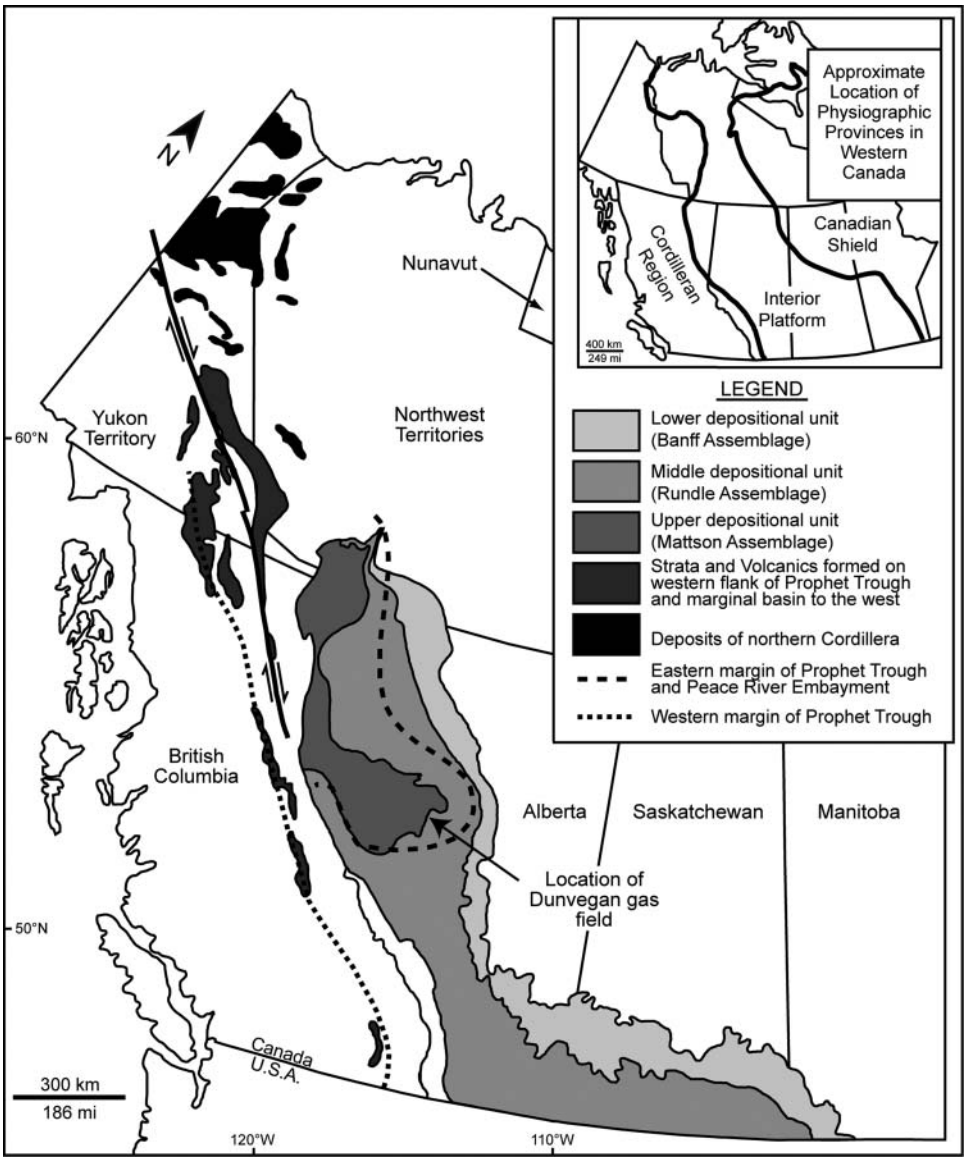

FIG. 2. A map of western Canada showing the depositional limits for sedimentation during the Mississippian and Pennsylvanian (Carboniferous Period). Non-highlighted areas denote positive regions where sediments are not preserved. The location of interest for this study is situated in the southeastern margin of the Peace River Embayment. The Debolt Formation corresponds to middle depositional unit (Rundle Assemblage) deposited during the Visean. Inset shows the main physiographic provinces of western Canada. Figure modified from Richards et al. (1993, 1994).

Despite providing expressible topographic relief from the Cambrian to Devonian, a combination of subsidence (compression and extension) and normal faulting (horst and graben structures) to the Peace River Arch during the mid-Devonian to Permian provided locations for sediments to accumulate (Cant, 1988; O'Connell et al., 1990). As a result of subsidence and normal faulting, the Peace River Arch became a negative feature from the Mississippian to Jurassic (Hein, 1999). Isopach maps of northwestern Alberta show the Debolt Formation to be the thickest in areas interpreted to be bounded by extensional faults (Cant, 1988). The Peace River Embayment may have become connected to the Prophet Trough during the early- and middle-Tournaisian due to the faulting and regional subsidence that continued throughout the Mississippian and Pennsylvanian (Durocher and Al-Aasm, 1997). Connection with the Prophet Trough helped facilitate deposition of a thick succession within the embayment and across the western Canadian Cratonic Platform (O'Connell et al., 1990). As a result of these aforementioned events, both stratigraphic (anhydrite, shale accumulations, pinch-outs of dolomitized burrow intervals) and structural (two-way up dip closures) petroleum traps formed within the Dunvegan gas field (Cioppa et al., 2003).

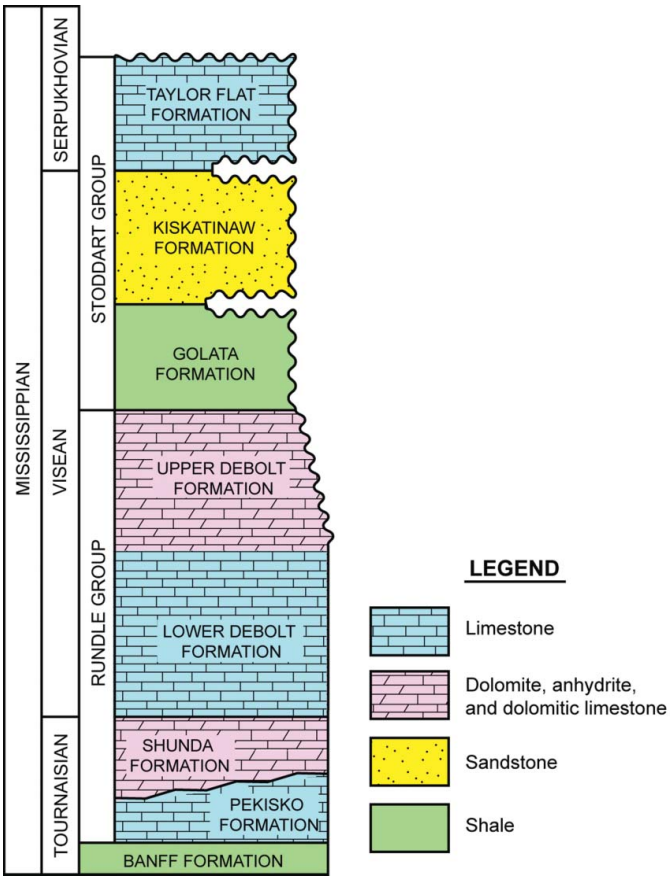

FIG. 3. Subsurface stratigraphic column of the Mississippian Period for the Peace River Embayment of northwestern Alberta and interior platform of northeastern British Columbia (after Richards et al., 1993; Durocher and Al-Aasm, 1997).

STRATIGRAPHIC SETTING

The Mississippian succession in the Peace River Embayment of northwestern Alberta and interior platform of northeastern British Columbia is subdivided into three main stratigraphic units. In chronological order, these units include (i) lower to middle Tournaisian Banff Formation, (ii) middle Tournaisian to upper Visean Rundle Group, and (iii) upper Visean to Serpukhovian Stoddart Group (O'Connell, 1994) (Fig. 3). The Debolt Formation is Visean in age and belongs to the Rundle Group. Consisting primarily of carbonate and evaporitic facies, the Debolt Formation typically grades into deeper basinal facies towards the west (Richards, 1989; Durocher and Al-Aasm, 1997; Al-Aasm and Packard, 2000). Macauley (1958) was the first to subdivide the Debolt Formation into lower and upper members. Law (1981) later subdivided the Debolt Formation into five informal members in northeastern British Columbia. The Debolt Formation is 244 m thick at its type section in west-central Alberta and becomes progressively thinner near its southwestern depositional limit (Richards et al., 1993). Within the Peace River Embayment, the Debolt Formation overlies the Shunda Formation in the east and the Pekisko Shale (Formation F) in the west (Richards et al., 1993). The Golata Formation disconformably overlies the Debolt Formation throughout the embayment. The outcrop nomenclature of the Mount Head and Livingstone formations have been applied to internal zones of the Debolt Formation with varying degrees of success (Packard et al., 2004).

In general, the Debolt Formation records no less than 30 shoaling-upward hemicycles or fourth/fifth order parasequences (Al-Aasm and Packard, 2000; Packard et al., 2004). These numerous packages are a reflection of the ongoing relative sea level oscillation in a shallow-water to littoral setting during the Visean. In Alberta, an early Visean transgression is recorded by the presence of protected-shelf carbonates in the basal part of the Debolt Formation above the restricted-shelf carbonates of the Shunda Formation (Packard et al., 2004). The subsequent regression, recorded by anhydrite and restricted-shelf carbonates preserved in the upper Debolt Formation of west-central Alberta and east-central British Columbia, appears to have coincided with sedimentation of the regressive Wileman and Salter members of the Mount Head Formation (Richards et al., 1993). Towards the east and east-southeast into Alberta, the upper member of the Debolt Formation becomes anhydritic and displays sabkha cycles. Reservoir zones in the Dunvegan gas field are located in the uppermost argillaceous unit (Al-Aasm and Packard, 2000). This argillaceous unit consists of a succession of stacked sabkha cycles of thinly interstratified carbonates, evaporites, and siliclastics, which are individually less than 2 m thick (Al-Aasm and Packard, 2000). A stratigraphic cross-section (Fig. 4) along a transect through the Dunvegan gas field illustrates the cyclical nature of the sabkha cycles.

DATABASE AND METHODS

In this study, 15 drill cores from the Dunvegan gas field were examined (see Fig. 1) along with 30 thin sections. The thin sections from the drill core samples were examined under a polarizing microscope. Sedimentological characterization included identification of carbonate grains (e.g., ooids, pisoids, oncoids, and other allochems), fossils, bedding contacts, layer thicknesses, primary and secondary physical structures, lithologic constituents, and accessory minerals. Ichnological data comprised descriptions of ichnogenera, cross-cutting relationships, and bioturbation intensity.

Isotopic analyses ($\delta^{18}O$ and $\delta^{13}C$) were performed on the burrow fill and surrounding matrices. Samples for isotopic analysis were obtained from representative sections of slabbed core and were mechanically extracted using the engraver tip of a high-speed rotary drill. The samples were selectively obtained from locations where discrete burrows were present or where burrows were absent (i.e., matrix). In each case, 10 to 25 mg samples were excavated from a depth of around 1 to 2 mm. In the case of burrow samples, this occasionally

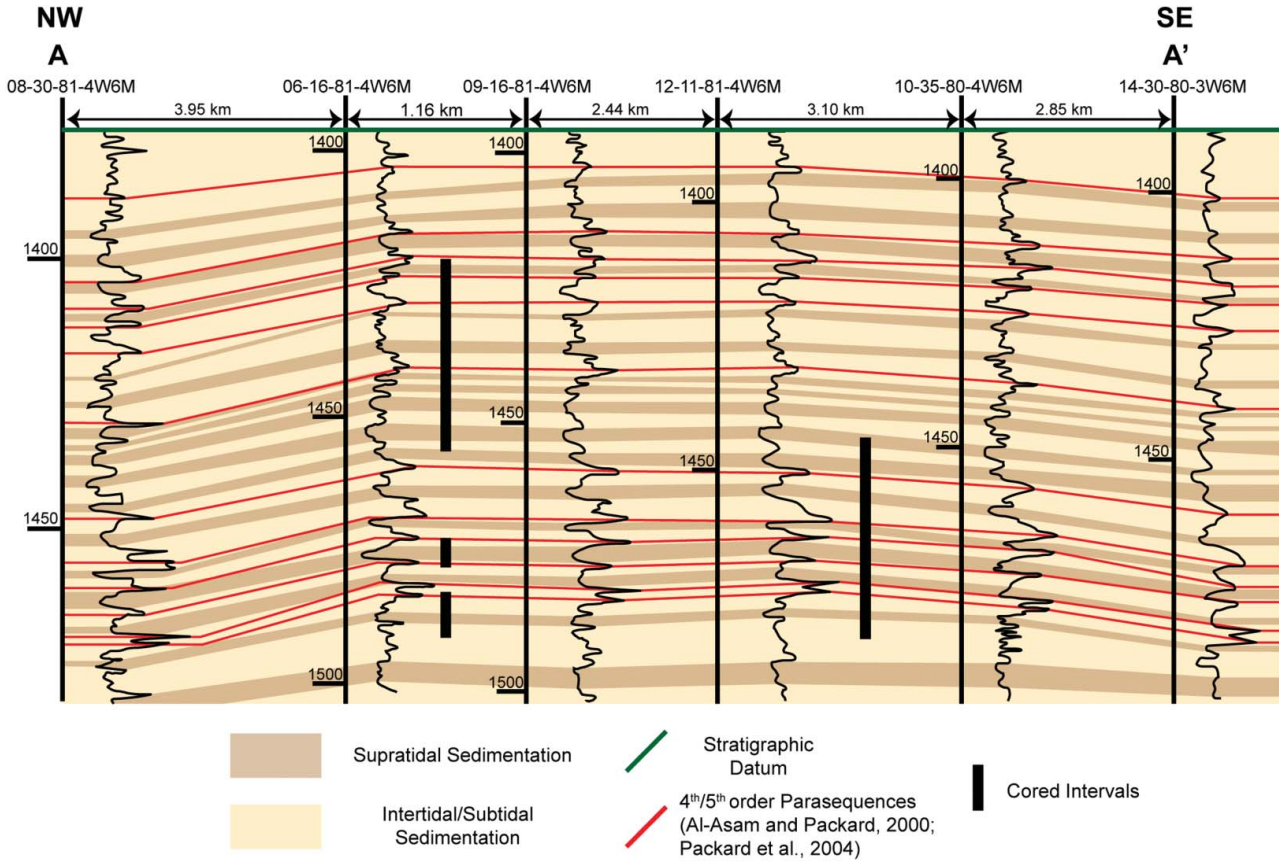

FIG. 4. Stratigraphic cross-section of the Debolt Formation along the northwestern part of the Dunvegan gas field. All well-logs shown are gamma ray. Twelve parasequence surfaces are recognized in this cross-section and are commonly represented in core as thinly bedded shale surfaces. Within these parasequences are stacked sabkha facies that are gradational with tidal flat, lagoonal, and shoal sediments. The repetitive nature of these facies over a large stratigraphic interval indicates high levels of sea level oscillation (i.e., transgressive-regressive cycles) in a shallow-water ramp setting during the Visean. (See Color Plate II.)

necessitated sampling more than one burrow in an interval. Samples for the isotopic analysis of the calcite phase were obtained by reaction with 100% phosphoric acid (H_3PO_4) for one hour at 25°C using the technique outlined by McCrea (1950). Samples for the isotopic analysis of the dolomite phase were obtained after an additional 24 hours in 100% H_3PO_4 at 50°C. Isotopic analyses were performed with a Finnigan-MAT 252 mass spectrometer operated in dual inlet mode. All isotopic values are reported in standard delta notation (δ) relative to PDB standards (Craig, 1957).

RESULTS

Facies Analysis

In this study, the Dunvegan gas field can be subdivided into six reoccurring facies intervals: nodular and bedded anhydrite (Facies 1), microbially laminated mudstones (Facies 2), massive-patterned mudstone (Facies 3), bioturbated mudstone-wackestone (Facies 4), skeletal packstone-wackestone (Facies 5), and peloidal grainstone-packstone (Facies 6). Within the study area, Al-Aasm and Packard (2000) identified oxidized muds and highly bioturbated sediments as the main intervals with dolomite present. In this context, the bioturbated mudstones-wackestones (Facies 4) represents the primary focus for this study regarding petrographic and isotopic analysis.

Facies 1 (F1): Nodular and Bedded Anhydrite

Description. Facies 1 consists of dense anhydrite and anhydritic-dolomite that is nonbioturbated. The most commonly observed type of anhydrite is nodular, with mottled and cryptocrystalline fabrics and occasional dolostone stringers. Nodules vary from 1 to 6 cm in diameter and are ovoid to irregular in shape (Figs. 5A-B). Facies 1 is typically embedded within dolostone and commonly has thicknesses ranging from 10 to 30 cm. Expressions of anhydrite in subvertically elongated position, with crystals ranging up to 10 cm in length, are also present (Fig. 5C). Examples of more massive nodular anhydrite, reaching up to 2 m in thickness, also occur within F1. This unit contains larger nodules (up to 10 cm) and typically contains little matrix. In areas, the nodules are present within, or juxtaposed, to stylolites or pressure dissolution seams

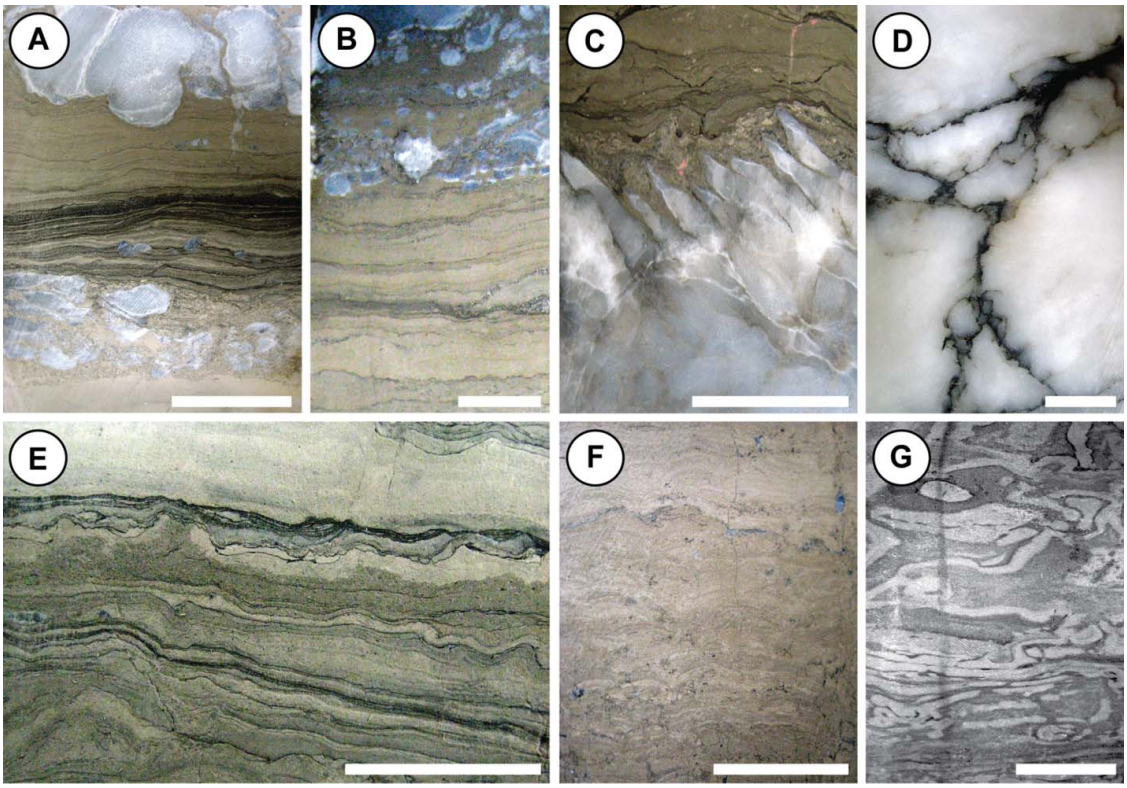

FIG. 5. Core photographs of supratidal to intertidal facies in the Dunvegan gas field. All scale bars are 3 cm. **A.** Eroded nodular anhydrite capped by planar to wavy black shale and laminated mudstone. The biolaminated mudstone is sharply overlain by nodular anhydrite. Well 12-11-81-4W6M, depth 1479.83m. **B.** Laminated mudstone overlain by nodular anhydrite. Well 5-16-80-3W6M, depth 1478.10m. **C.** Subvertically elongated nodular anhydrite in an argillaceous, brown-colored dolomitic mudstone matrix capped by massive appearing dolomudstone with dissolution seems. Well 7-18-80-3W6M, depth 1472.80m. **D.** Nodular mosaic anhydrite of chicken-wire juxtaposed to stylolites and interstitial mud. Well 9-25-81-5W6M, depth 1601.50m. **E.** Bio-laminations with wavy to contorted laminae, dark organic-rich partings, and stylolites. Well 7-3-81-4W6M, depth 1480.54m. **F.** Domal stromatolites. Well 7-3-81-4W6M, depth 1487.65m. **G.** Massive patterned cryptocrystalline mudstone with alternating dark- and light-colored fabrics. Well 7-15-80-3W6M, depth 1474.52m. (See Color Plate III.)

(Fig. 5D). Examples of bedded anhydrite containing thin interbeds of dolostone are also present in localized areas. These bedded anhydrites range up to 10 m in thickness and preserve planar to wavy laminations. Where dolomite is present, it is typically expressed as millimeter- to centimeter-thick laminae or thin discontinuous beds.

Interpretation. The combination of different anhydrite morphologies suggests deposition within closely related environments along an arid marine coastline. Given the large range of nodular fabrics, it is likely that the nodular anhydrite is indicative of a sabkha environment. It is important to note, however, that not all nodular anhydrite is formed in a sabkha setting (Warren and Kendall, 1985). The presence of isolated masses of nodular (chicken-wire) anhydrite within other carbonates indicates displacive growth of gypsum and anhydrite in the upper zones of a sabkha (Warren and Kendall, 1985; Kendall, 2010). Similarly, examples of more massive nodular anhydrite indicate that they represent an overprinted subaqueous (salina) gypsum deposit (Kendall, 2010). The subvertical elongated morphology of anhydrite nodules further indicates subaqueous precipitation of gypsum in either shallow (less than 10 m) hypersaline lagoons or brine ponds adjacent to the sabkha (Warren and Kendall, 1985). Additional evidence of subaqueous sedimentation is provided by the bedded anhydrite with interbeds of dolostone. The nature of the anhydrite, with little evidence of subaerial exposure, implies diagenetic alteration of primary gypsum that chemically precipitated under subaqueous conditions (Hardie, 2003). The presence of stylolites and pressure dissolution seams in some examples implies that some nodular anhydrite formed during burial at depths of tens to several hundred meters (Machel and Burton, 1991; Machel, 1993).

Facies 2 (F2): Microbially Laminated Mudstones

Description. Facies 2 consists of tan-colored, cryptocrystalline, microbially laminated carbonate mudstones (Fig. 5E). Present within these laminated mudstones are very fine, dark-brown to black, organic-rich laminae that vary from 5 to 50 cm in thickness. Sedimentary structures include irregular to planar laminations and low-relief domal stromatolites (Fig. 5F). Petrography of F2 shows the presence of silt-sized to fine-grained sandstones within the matrix. These grains are typically sub-rounded to sub-angular and occasionally form

bedded deposits. Subaerial exposure features include desiccation cracks and some fenestral (birds-eye) porosity. Skeletal fragments and bioturbation are extremely rare in F2.

Interpretation. Fenestral porosity, formed by a combination of gas bubbles and sediment shrinkage, are common occurrences in tidal-flat carbonates (Choquette and Prey, 1970). Combined with the presence of desiccation cracks, periodic subaerial exposure of the substrate is envisioned in F2. The presence of low-relief domal stromatolites also suggests deposition on high intertidal and supratidal sites and on tidal flats with protected shorelines (Logan, 1961; Davies, 1970; Taylor and Halley, 1974). Due to shoreline isolation, fluctuating salinities were probable, thereby presenting additional ecological stresses to the localized macrofauna. Because most eukaryotic organisms are unable to withstand high salinities or exposure to extreme salinity fluctuations (Franks and Stolz, 2009), the levels of bioturbation and overall fossil content are expectedly limited in F2.

As a result of extreme physico-chemical conditions, flat laminated microbial mats were able to flourish in the intertidal flats and hypersaline lagoons of the carbonate ramp (Nicholson et al., 1987; Stolz, 1990). The presence of organic laminae is attributable to the sharp geochemical interface present beneath the microbial mat (Krumbein and Cohen, 1977). Pore waters below the interface were anoxic and thus had a higher preservation potential for buried organic matter. The presence of siliciclastic material within the microbial mats is likely the result of sticky EPS produced by microorganisms (Krumbein, 1994). As shown in the Mellum Island, southern North Sea and southern coast of Tunisia (Gerdes et al., 2000), microbial mats coated with EPS have the ability to trap and bind sediment introduced into the tidal flats.

Facies 3 (F3): Massive Patterned Mudstone

Description. Facies 3 is recognizable in core by its distinctive mottled fabric (Fig. 5G). In short, F3 is a cryptocrystalline dolomudstone that contains no visible burrows or fossiliferous material. Facies 3 ranges in thickness from 10 to 30 cm, with some thicker intervals present. The mottled fabric consists of a pattern of light- and dark-colored areas, with the concentration of pyrite crystals seen in the darker regions. Facies 3 is commonly gradational with F1, F2, and F4, and is observable throughout the Dunvegan gas field.

Interpretation. The variable size, irregular shape, and indistinct contacts of the mottles suggest they are not related to burrowing. Instead, the alteration of light- and dark-colored fabrics represents a diagenetic feature wherein microcrystalline pyrite became concentrated in the darker regions (Dixon, 1976; Kendall, 1977b; Kirkham, 2004). Termed "patterned carbonate" by Dixon (1976), the diagenetic origin of this unique fabric is attributable to the destruction of calcium sulfate nodules by sulfate-reducing microorganisms, thereby leading to pyrite formation (Kendall, 1977b). Within reducing subenvironments, the formation of pyrite commonly requires pH values greater than 8.0 and salinities above 200‰ (Krumbein and Garrels, 1952). Such extreme conditions suggest sedimentation of F3 within a restricted supratidal to intertidal setting (Dixon, 1976), similar to those observed in the modern Persian Gulf (e.g., Butler, 1969). Furthermore, the cryptocrystalline dolomudstone suggests formation under hypersaline conditions with precipitation likely induced by sulfate-reducing bacteria (Kirkham, 2004).

Facies 4 (F4): Bioturbated Mudstone-Wackestone

Description. Bioturbated dolomudstones-dolowackestones (60 to 100% of total reservoir volume) represent important reservoir strata within the Dunvegan gas field. Common assemblages include monospecific examples *Chondrites, Quebecichnus*, and *Planolites* (Figs. 6A-B). Other ichnofossils occasionally dispersed within F4 include moderately abundant *Thalassinoides* (Fig. 6C), rare *Arenicolites*, rare *Skolithos*, and very rare *Zoophycos*. Although no fossil fragments are visible in core, petrographic sections reveal low to moderate fossil content composed of benthic invertebrates and calcareous algae that have been completely reworked by bioturbation. Gradational with F2 and F3, F4 has thicknesses on the order of decimeter to meter scale.

Interpretation. The predominance of low-diversity ichnological assemblages is typical of ecological stresses, such as high salinity and low oxygenation, commonly present within lagoonal settings (MacEachern et al., 2007). For example, it has been shown that the ghost shrimp *Callianassa californiensis*, which make *Thalassinoides*-type burrows, is capable of tolerating fluctuating salinities (Thompson and Pritchard, 1969). Complex feeding traces (i.e., fodinichnia) are also abundant within oxygen-poor environments (Bromley and Ekdale, 1984; Ekdale, 1988; Ekdale and Mason, 1988). *Chondrites*, for example, is believed to be unique to anoxic conditions (Bromley and Ekdale, 1984). The presence of *Zoophycos* may reflect the activity of opportunistic organisms habituating poorly oxygenated communities (Ekdale, 1988; Ekdale and Lewis, 1991; Miller, 1991). Increased ichnodiversity present within some intervals in F4 (e.g., *Skolithos*, *Arenicolites*) is interpreted to be the result of events such as fresh water influx that helped alleviate earlier stresses imparted on the ecosystem. Collectively, F4 represents a restricted, low-energy lagoon.

Facies 5 (F5): Skeletal Packstone-Wackestone

Description. Facies 5 is a bioclastic packstone-wackestone composed of a diverse assemblage of fauna (Fig. 6D). Identifiable fossils include fragmented brachiopods, crinoids, bryozoans, and ostracodes. Also present are stylolites, pressure dissolution seams, and peloids. Grain sorting varies between different intervals, ranging from poorly sorted to well sorted. The matrix is composed primarily of carbonate mud within the wackestone successions, and becomes increasing depleted of mud in the more well-sorted packstone-rich intervals. Either gradational or sharp contact with F2, F3, and F4, bed

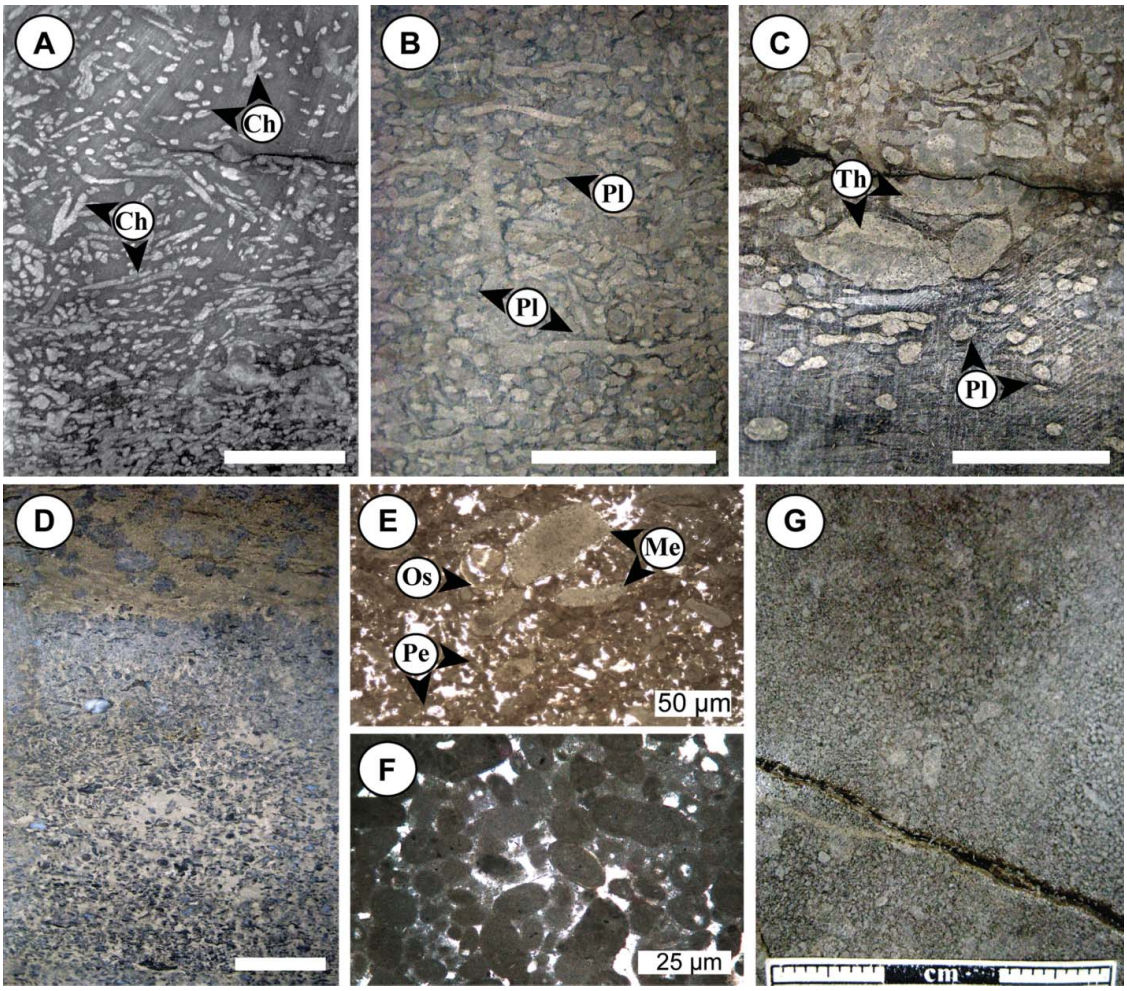

FIG. 6. Core photographs of subtidal Debolt Formation facies in the Dunvegan gas field. All scale bars are 3 cm unless otherwise noted. **A.** Highly bioturbated, monospecific assemblage of *Chondrites* (Ch). Well 8-13-81-5W6M, depth 1452.31m. **B.** Highly bioturbated dolomudstone dominated by a monospecific assemblage of *Planolites* (Pl). The interval forms the principal reservoir in the observed well, with permeabilities ranging above 40 mD. Well 9-18-81-4W6M, depth 1412.15m. **C.** Bioturbated assemblage of *Planolites* (Pl) and *Thalassinoides* (Th). Well 8-20-80-3W6M, depth 1497.25 m. **D.** Fossiliferous packstone overlain by laminated mudstone with metasomatic anhydrite. Fossils include crinoids, brachiopods, bryozoans, and ostracodes. Well 7-15-80-3W6M, depth 1439.64m. **E.** Thin section photomicrograph of peloidal grainstone facies (Pe), where the irregular shape suggest they may have been originally skeletal grainstones. Subordinate amounts of ostracode (Os) and crinoids fragments exist and some of the larger grains display simple micrite envelopes (Me). Calcite cement occludes primary porosity. Well 8-13-81-5W6M, depth 1455.02m. **F.** Thin section photomicrograph of peloidal grainstone facies, where the rounded character of the grains suggests fecal pellets. Calcite cement occludes primary porosity. Well 5-16-80-3W6M, depth 1457.20m. **G.** Massive bedded deposit of peloidal grainstone. Well 7-3-81-4W6M, depth 1492.25m. (See Color Plate IV.)

thicknesses in F5 range from 10 to 25 cm, although thicker intervals are present.

Interpretation. The diversity of fossils suggests a normal-marine origin (James and Kendall, 1992). The well-sorted, fine-grained, bedded nature indicates that the skeletal material underwent earlier wave reworking in a high-energy beach or shoal environment. The fact that F5 is in close contact with multiple facies (F2, F3, F4) suggests possible allochthonous transportation of sediment (e.g., tempestites). As a result, sedimentation of these skeletal packstones-wackestones may have been due to either storm activity or minor sea level transgressions that inundated the restricted intertidal to subtidal regions of the lagoonal environment.

Facies 6 (F6): Peloidal Grainstone-Packstone

Description. Facies 6 consists of a peloidal grainstone-packstone. Allochems include oncoids, ooids, and pisoids. Micritic envelopes (Fig. 6E) have been identified on pisoids and shell fragments. The peloids range in shape from ovoid (Fig. 6F) to nonrounded. Comprising a poor to moderately diverse assemblage of skeletal fragments, bioclasts include ostracodes, crinoids, brachiopods, and bryozoans. The majority of the intervals are massive bedded (Fig. 6G), although low-angle cross-bedding is present in places. Bioturbation is generally preserved locally as indistinct mottling. Gradational with F4 and F5, F6 has a thickness ranging from 30 cm to 1 m.

Interpretation. The presence of irregularly shaped peloids suggests micritization of allochems, such as skeletal fragments or ooids (Bathurst, 1966). Peloids that are either elongated or ovoid in shape suggests a fecal origin (Land and Moore, 1980). Preservation of the peloids indicates deposition within a shallow, low-energy, restricted marine environment (Enos, 1983). Due to the presence of low-angle cross bedding and fragmented fossils, F6 is interpreted to have accumulated in either shallow peloidal shoals or low-relief banks in restricted lagoonal environments (Qing and Nimegeers, 2008).

Petrographic Analysis

Petrographic analysis of the bioturbated fabrics (Facies 4) is shown in Figures 7A–D. The dolomite-filled burrows, 0.5 to 2 cm in diameter, commonly contain dolomite crystal sizes ranging from 1 to 35 microns, with an average size of 10 to 15 microns. The dolomite forms microsucrosic (planar-E) fabrics (after Sibley and Gregg, 1987) and is generally euhedral. Dolomitization within the burrows is generally thorough and a sharp contact commonly exists between the burrow-associated dolomite and calcite matrix. Furthermore, it appears that the microcrystalline dolomite within the burrows has been largely preserved and not altered by burial diagenesis. Similarities in textural composition with dolomites from the Holocene Abu Dhabi sabkhas (McKenzie, 1981) help support this observation.

The majority of calcite within the burrows is consistent with cement precipitated in a marine environment (e.g., blocky calcite spar). The lime mudstone-wackestone surrounding the burrows is dominantly fine-matrix sediment that contains minor amounts of disarticulated and fragmented allochems. Dolomite crystals within the matrix are similar to those observed within the burrows, suggesting residual burrow pathways that were dolomitized.

Geochemistry

Isotopic analyses of calcites and dolomites are shown in Figure 8. To represent the relationship between the calcite and dolomite isotopes within the burrows and matrix, a straight line ($y = mx + b$) was employed. From this equation, the coefficient of determination, R^2, can be deduced. In short, the closer the R^2 is to + 1 or -1, the better the correlation between the isotopes being analyzed. Using R^2, the calcite and dolomite plotted as linear trends with good correlations (i.e., $R^2 > 0.62$), thereby indicating a strong linear relationship for the calcite and dolomite isotopes regardless of sample location (i.e., burrow or matrix).

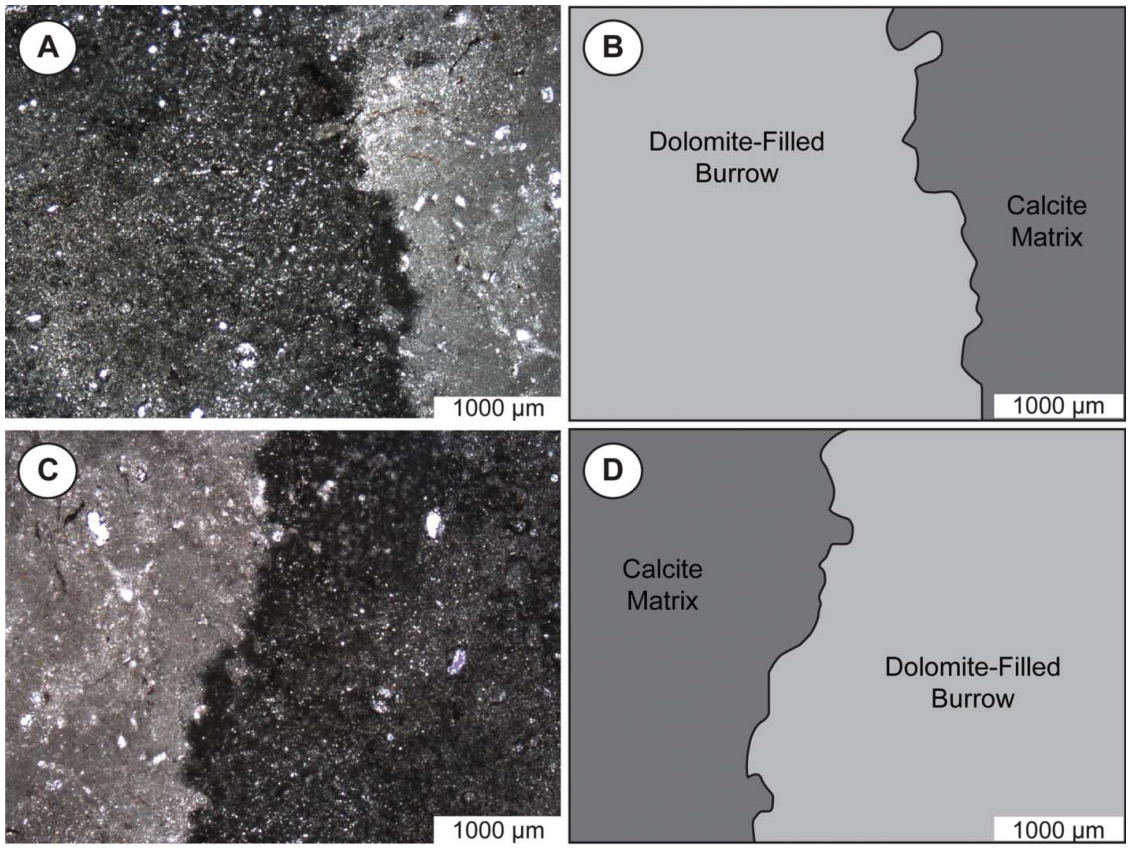

FIG. 7. Thin section photomicrographs **(A, C)** and corresponding schematic diagrams **(B, D)** of dolomite-filled burrows and their surrounding calcite matrices. Both thin section photomicrographs are from Well 9-18-81-4W6M, depth 1412.15m.

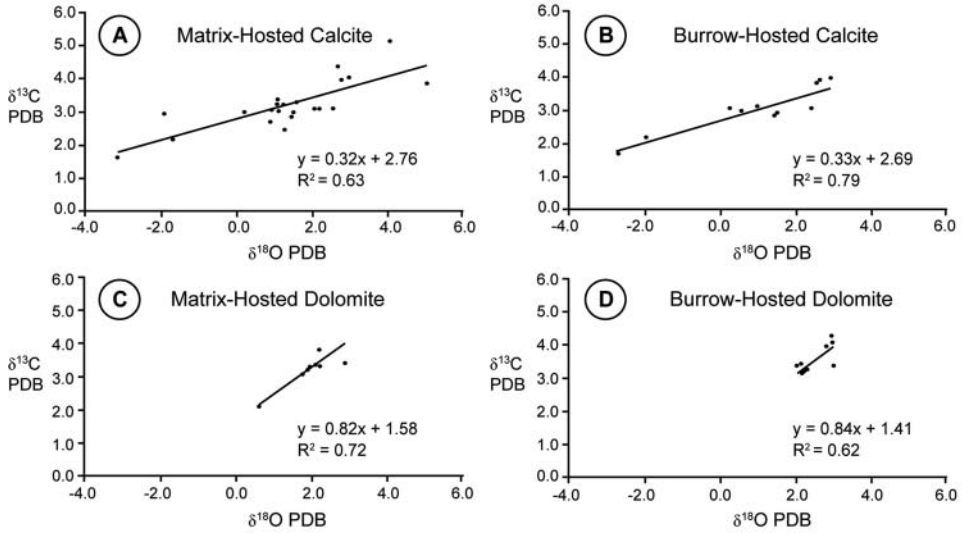

FIG. 8. Isotopic values for calcite and dolomite from the burrows and adjacent matrix. **A.** Matrix-hosted calcite (n = 22) has a $\delta^{13}C$ mean of 3.2‰ and $\delta^{18}O$ mean of 1.4‰. **B.** Burrow-hosted calcite (n = 13) has a $\delta^{13}C$ mean 3.1‰ and $\delta^{18}O$ mean of 1.1‰. **C.** Matrix-hosted dolomite (n = 12) has a $\delta^{13}C$ mean of 3.4‰ and $\delta^{18}O$ mean of 2.1‰. **D.** Burrow-hosted dolomite (n = 13) has a $\delta^{13}C$ mean 3.5‰ and $\delta^{18}O$ mean of 2.4‰.

Calcite isotopic ratios

Matrix calcite (n = 22) has measured $\delta^{13}C$ values ranging from 1.6 to 5.1‰ (mean = 3.2‰) and $\delta^{18}O$ values of −3.1 to 5.0‰ (mean = 1.4‰). A similar range of values is observed for burrow-hosted calcite (n = 13), where $\delta^{13}C$ range from 1.7 to 4.0‰ (mean = 3.1‰) and $\delta^{18}O$ range from −2.7 to 2.9‰ (mean = 1.1‰). The slope for matrix-hosted calcite (Fig. 8A) differs only slightly from that of burrow-hosted calcite (Fig. 8B), with values of 0.32 and 0.33 calculated for matrix- and burrow-hosted, respectively.

Dolomite isotopic ratios

The $\delta^{13}C$ for dolomite ranges from 3.1 to 4.6‰ (mean = 3.4‰) and 3.2 to 4.3‰ (mean = 3.5‰) for samples obtained from the matrix (n = 12) and burrows (n = 25), respectively. In comparison to calcite, dolomite tends to be more enriched in $\delta^{18}O$, with a narrower range of isotopic ratios is observed. For matrix dolomite, $\delta^{18}O$ ranges from 0.7 to 2.9‰ (mean = 2.1‰), and $\delta^{18}O$ for burrow-hosted dolomite between 2.1 and 2.4‰ (mean = 2.4‰). An even smaller difference in calculated slopes is present for the dolomite phases, with values of 0.82 and 0.84 for matrix-hosted (Fig. 8C) and burrow-hosted (Fig. 8D), respectively.

DISCUSSION

Paleoenvironmental Reconstruction

The carbonate facies within the Dunvegan gas field are comparable to the modern intertidal flats and sabkhas of the Persian Gulf (Evans, 1966; Butler, 1969; Behairy et al., 1991; Al-Youssef et al., 2006) and the Upper Cretaceous intertidal facies of Hvar Island, Croatia (Diedrich et al., 2011). The six facies described correspond to the shallow inner and middle portions of the carbonate ramp (Fig. 9). They extend from the peritidal setting to the shallow subtidal zone through a low to moderate energy carbonate shoal facies. Core analysis shows mainly gradational boundaries within the facies, suggesting that they are genetically related and demonstrate a low depositional gradient. For Facies 5 demonstrating an allochthonous origin, tempestites are envisioned as a possible mechanism for sediment transportation along the shallow-gradient ramp.

The lithofacies cycles in the Dunvegan gas field, commonly capped by nodular to nodular mosaic anhydrite, are interpreted as fourth and fifth order transgressive-regressive parasequences that represent the initial flooding and subsequent progradation of a sabkha system (Al-Aasm and Packard, 2000; Packard et al., 2004). The presence of laminated, vertically elongated, and massive nodular anhydrite, as described in F1, suggests numerous other evaporitic sub-environments existed in the backshore adjacent to the sabkha shoreline, such as hypersaline lagoons. The lagoonal facies are characterized by massive, highly bioturbated packstone, wackestone, and mudstone lithofacies. The thin packstone/wackestone beds that were occasionally present between more massive wackestones and mudstones may represent possible storm deposits.

Monospecific assemblages of ichnofossils, formation of patterned carbonate, and lack of tidal structures, among other features, supports the interpretation that the lagoon was restricted. Isolating the lagoon from the open marine water was peloidal shoals/low-relief banks composed of fecal material and skeletal fragments. As the geochemical results shows,

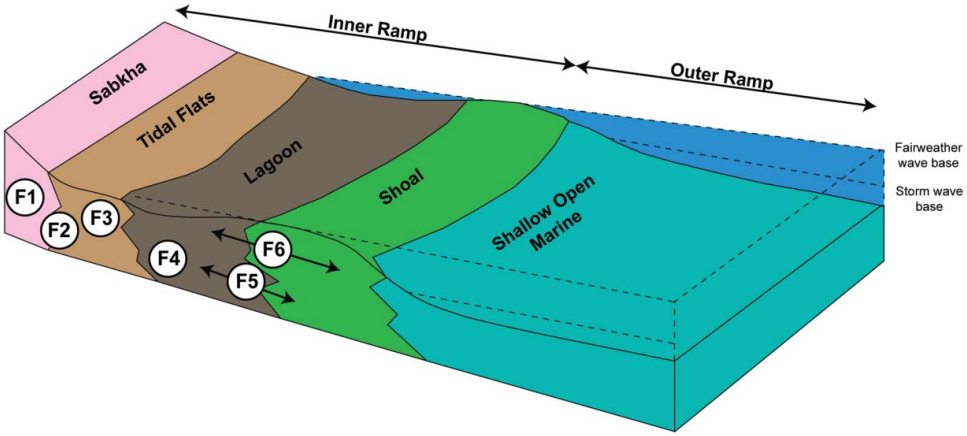

FIG. 9. A schematic drawing of a low-angle carbonate ramp reflective of sedimentation during the Visean within the Dunvegan gas field. Superimposed on the carbonate ramp is the location of the six facies identified during core logging. Facies 4 (bioturbated mudstone-wackestone) occurs primarily within the lagoonal portions of the inner ramp and represents the primary reservoir intervals.

an abundance of organic carbon (burrows, biolaminated mudstones, EPS), coupled with periods of anoxia within the restricted lagoon, provided favorable conditions for the development of dolomitization.

Dolomitization Models

The $\delta^{13}C$ (3.4‰ matrix, 3.5‰ burrows) and $\delta^{18}O$ (2.1‰ matrix, 2.4‰ burrows) values for the early matrix dolomite in this study are consistent with precipitation from hypersaline marine fluids, as observed elsewhere by Al-Aasm (2000), Al-Aasm and Packard (2000), and Cioppa et al. (2003) within the Dunvegan gas field. The Mg-rich brines, likely derived from Mississippian seawater (Bruckschen et al., 1999; Cioppa et al., 2003), resulted in the replacement of carbonate mud by the early matrix dolomite and precipitation of primary evaporites. Correlation of isotopic values in this study with Holocene dolomites from the Abu Dhabi sabkhas (McKenzie, 1981) support this assertion (Fig. 10). Because of the evidence supporting sabkha dolomitization, it is likely that other models of dolomitization have been overlooked within the Dunvegan gas field.

In this context, it must also be noted that recrystallization, due to burial diagenesis, does not appear to have had any significant impact on the texture or geochemical values of the microcrystalline dolomites preserved within the burrow fabrics. This is unique, given that the Debolt Formation within the Dunvegan gas field has undergone over 300 million years of burial history to depths of roughly 4 km and temperatures in excess of 100°C (Al-Aasm, 2000; Al-Aasm and Packard, 2000). It has been postulated by Al-Aasm (2000), Al-Aasm and Packard (2000), and Packard et al. (2004) that hydrodynamic isolation, geochemically closed diagenetic systems, and hydrocarbon charging each played a significant role in helping preserve the microcrystalline dolomite. The exact mechanism, however, remains up for debate.

Given the data presented above, burrow-mediated dolomitization is being asserted in this study as an *additional* dolomite-promoting mechanism. This is because we ascribe the compositional differences observed in the isotopic distributions to reflect the different biogeochemical processes occurring within and adjacent to the burrows (Gingras et al., 2004; Konhauser and Gingras, 2007, 2011; Rameil, 2008; Lalonde et al., 2010; Petrash et al., 2011; Corlett and Jones, 2012).

Parameters Influencing Dolomitization

When the isotopic values for calcite and dolomite are plotted together (Fig. 10), the linear trend observed for calcite is maintained and the dolomite values fall into two general groups either above or below the calcite linear trend. These two fields likely represent dolomite that has precipitated in different spatial environments within the carbonate ramp. The scale of these spatial differences is currently unclear.

The zone of relative enrichment of $\delta^{13}C$ in dolomite (i.e., values occurring above the calcite linear trend) is consistent with a biogenically mediated phase. $\delta^{13}C$ enrichment has been interpreted as being associated with methanogenesis (Roberts et al., 2004) and with conditions of anaerobic fermentation (Reitsema, 1980; Dimitrakopoulos and Muehlenbachs, 1987).

An overall enrichment of $\delta^{18}O$ in dolomite relative to calcite suggests that the pore-water associated with dolomitization may have been enriched in $\delta^{18}O$ due to evaporitic and sabkha conditions or due to the dolomite undergoing a greater fractionation factor relative to calcite. Low-temperature experiments of modern dolomite precipitating in equilibrium with calcite under conditions of MSR indicate that dolomite should be enriched in $\delta^{18}O$ by approximately 2.6‰ (Vasconcelos et al., 2005). Mean $\delta^{18}O$ values for dolomite in this study are enriched by 0.8‰ relative to mean calcite values (1.2‰). This fractionation is closer to values measured in a lab than

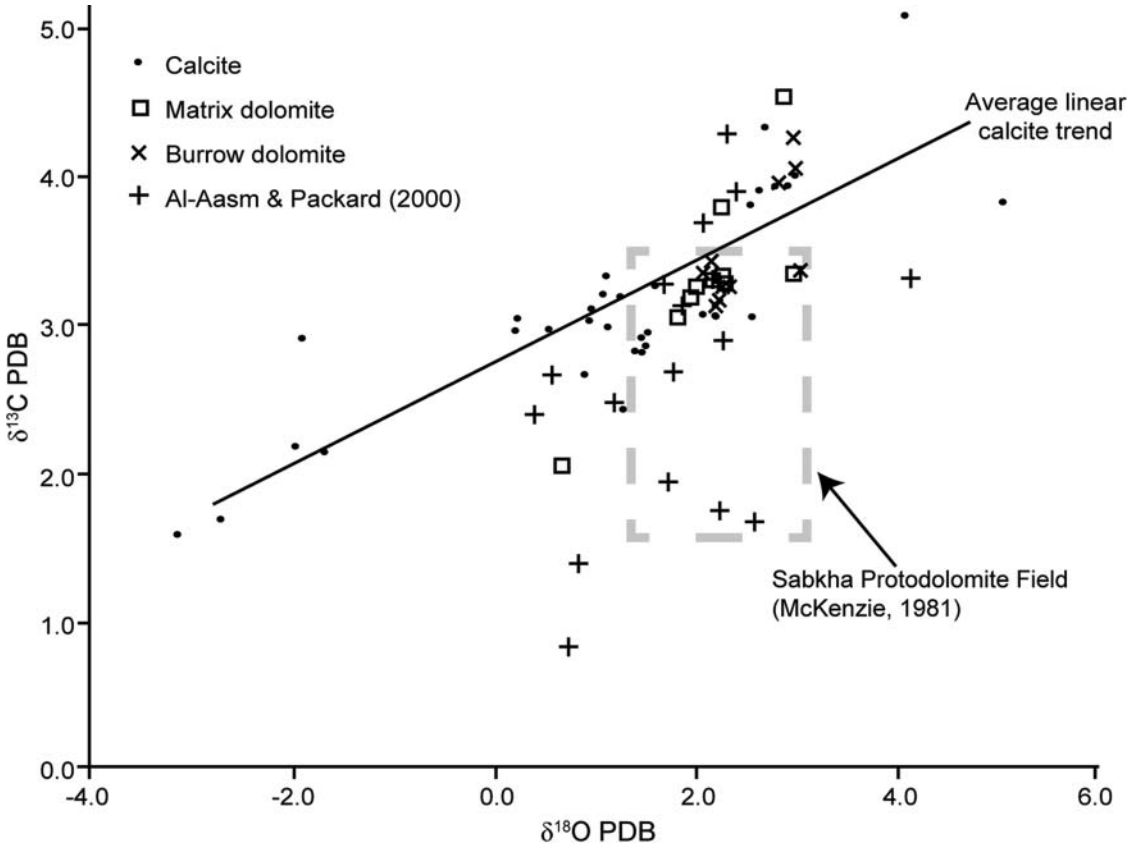

FIG. 10. Composite plot showing the average linear trend for calcite and the two distinct zones of dolomite occurring either above or below the calcite linear trend line. Observed $\delta^{18}O$ and $\delta^{13}C$ values from the burrow and matrix dolomites in this study are comparable to protodolomities values measured by McKenzie (1981) in the modern Abu Dhabi sabkhas and microdolomite values measured by Al-Aasm and Packard (2000) from the Dunvegan gas field.

values extrapolated to low-temperature conditions from high-temperature experiments (e.g., Epstein et al., 1964; Northrop and Clayton, 1966; O'Neill and Epstein, 1966). The similarity in approximated fractionation values calculated between calcite and dolomite in this study with those calculated by Vasconcelos et al. (2005) for dolomite and calcite precipitating from the same parent solution suggests that protodolomite precipitated in equilibrium with calcite rather than by replacement of pre-existing calcite.

There are examples of dolomitized burrows in the rock record, however, wherein $\delta^{18}O$ dolomite is depleted relative to calcite (e.g., Corlett and Jones, 2012). Within their study of burrow dolomites in the Middle Devonian Lonely Bay Formation in Northwest Territories, Canada, Corlett and Jones (2012) showed that a requisite for dolomitization, among others, was a high concentration of marine-dissolved organic matter. On the other hand, the burrows within the Debolt Formation lack marine-derived organic matter due to a sabkha based depositional setting.

As a result, a significant portion of the organic content within the Debolt Formation is most likely derived in part from the organisms and their by-products (i.e., fecal material, burrow wall linings) occurring within a lagoonal setting. Consequently, the distribution of $\delta^{18}O$ in dolomite relative to calcite within burrows, at present, appears to be influenced the source of organic matter and depositional setting. Clearly, further work needs to be completed to better define these boundaries throughout the geological rock record.

Less depleted $\delta^{13}C$ values within the burrow dolomites in the Dunvegan gas field are thought to result from dolomite formed either: (i) in association with early sulfate reduction (i.e., before pores become saturated with $\delta^{13}C$) or (ii) in sediments with little organic matter, where much of the CO_3^{2-} is derived from seawater (Compton, 1988; Mazzullo, 2000). It has been noted that $\delta^{13}C$ for dolomite precipitated in association with sulfate reduction in modern settings is initially very similar to $\delta^{13}C$ of calcite, but becomes progressively more depleted as sulfate-reducing conditions persist (Vasconcelos et al., 1995; Mazzullo, 2000). Studies of dolomite found associated with MSR in a modern lagoonal environment (e.g., Lagoa Vermelha, Brazil) suggest that dolomite is initially slightly $\delta^{13}C$ enriched relative to organic carbon, and becomes progressively depleted by as much as 5‰ upon shallow recrystallization (Vasconcelos and McKenzie, 1997). For this study, the majority of $\delta^{13}C$ values fall within 1‰ of seawater, although a few samples are as much as 2‰

lighter. The similarity of $\delta^{13}C$ values measured in the present study with those measured in modern field and laboratory dolomite associated with MSR suggest that the zone of isotopically light dolomite (i.e., values occurring below the linear calcite trend) most likely formed under early sulfate reducing conditions.

The high degree of similarity of burrow and matrix dolomite $\delta^{13}C$ to seawater values suggests that dolomite formed near the sediment-water interface, under conditions of early sulfate reduction. This is envisaged as occurring potentially within a burrow environment, where sulfate reduction can occur adjacent to or within a burrow (Waslenchuk et al., 1983). We therefore advocate that heterogeneities within the substrate, such as those made by bioturbation, helped promote dolomitization within the Dunvegan gas field.

The presence of anoxia within the lagoonal portions of the carbonate ramp is supported the presence of monospecific assemblages of burrows such as *Chondrites* and *Zoophycos* (Facies 4) (Bromley and Ekdale, 1984; Ekdale and Mason, 1988; Miller, 1991). High concentrations of pyrite (Facies 3) and organic matter preserved within the microbial mats (Facies 2) also confirm anoxic conditions. Given these geochemical conditions, it can be suggested that bottom seawater and uppermost sediment pore waters (i.e., burrowed zone) fluctuated from oxic to anoxic. The margins of the burrows walls, due to high organic carbon content, are also believed to have formed a localized reducing zone that allowed for MSR and localized dolomite precipitation.

From a reservoir viewpoint, early dolomitization was critical in preserving the micro-intercrystalline porosity within the burrow fabrics (Al-Aasm and Packard, 2000). Moreover, these dolomitized burrow fabrics commonly provide localized enhancement of permeabilities relative to the impermeable lime mud matrix. As shown by Gingras et al. (2007b, 2012) and Baniak et al. (2013), dolomitized bioturbated media commonly develop anisotropic permeability networks. Given the lateral extensiveness of these bioturbated intervals across the Dunvegan gas field (Fig. 4), proper identification of the dolomitized burrow fabrics is crucial to drilling success and optimal recovery.

CONCLUSIONS

In the Dunvegan gas field of northwestern Alberta, the Mississippian (Visean) Debolt Formation contains numerous indicators of sedimentation within a carbonate ramp setting. Among others, these include reoccurring intervals of patterned carbonate, monospecific assemblages of ichnofossils (e.g., *Chondrites*, *Planolites*), nodular anhydrite, biolaminated mudstones, and peloidal grainstones. The reduction of both fossils and burrows within the lagoonal settings indicates that physico-chemical stresses, such as reduced oxygen and fluctuating salinities, were prevalent during the Visean. These parasequence surfaces are laterally extensive and correlatable across the Dunvegan gas field.

Isotopically, the Dunvegan gas field provides an excellent example of early dolomitization within a sabkha setting. However, evidence for burrow-mediated dolomitization was also established when comparing calcite and dolomite isotope data from the burrows and adjacent matrix. The isotopic values for calcite follow a linear trend on a $\delta^{13}C$ versus $\delta^{18}O$ plot, while dolomite plots into two distinct zones either above or below the calcite linear trend. Dolomite that is $\delta^{13}C$ enriched relative to calcite is interpreted to be dolomite that formed in a zone of methanogenesis. The majority of dolomite measured, however, was depleted in $\delta^{13}C$ relative to average calcite values. This amount of isotopic depletion is similar to samples that are measured in laboratory and field-based studies where dolomite has been found in association with bacterial sulfate reduction coupled to the oxidation of organic carbon. High organic content, an essential component for MSR and subsequent near-surface dolomitization, is believed to have been derived in part from the organisms and their by-products (i.e., fecal material, burrow wall linings).

ACKNOWLEDGMENTS

We would like to thank Ichnos editor Luis Buatois, along with reviewers Hilary Corlett and Adrian Immenhauser, for their helpful comments and suggestions that improved the final version of this paper. Jenni Scott and David Morrow are acknowledged for their editorial input and helpful suggestions during earlier versions of this draft. We would like to thank Mark Labbe and David Pirie for their help regarding thin section preparation. The staff at the ERCB in Calgary, Alberta, is also recognized for their support and help during our stay at the core lab in summer 2010.

FUNDING

We are grateful for the financial support offered by ConocoPhillips, Devon Energy, and Statoil.

REFERENCES

Al-Aasm, I. S. 2000. Chemical and isotopic constraints for recrystallization of sedimentary dolomites from the Western Canada sedimentary basin. *Aquatic Geochemistry*, 6:227–248.

Al-Aasm, I. S. and Packard, J. J. 2000. Stabilization of early-formed dolomite: A tale of divergence from two Mississippian dolomites. *Sedimentary Geology*, 131:97–108.

Al-Youssef, M., Stow, D. A. V., and West, I. M. 2006. Salt Lake Area, northeastern part of Dukhan Sabkha, Qatar. *In* Khan, M. A., Böer, B., Kust, G. S., and Barth, H.-J. (eds.), Sabkha Ecosystems: Tasks for Vegetation Science (West and Central Asia). Springer, Netherlands, 42:163–181.

Aller, R. C. 1982. The effects of macrobenthos on chemical properties of marine sediment and overlying water. *In* McCall, P. L. and Tevesz, M. J. S. (eds.),

Animal-Sediment Relations: The Biogenic Alteration of Sediments. Plenum Press, New York, pp. 53–102.

Aller R. C. 1994. Bioturbation and remineralization of sedimentary organic matter: Effects of redox oscillation. *Chemical Geology*, 114:331–345.

Arvidson, R. S. and Mackenzie, F. T. 1999. The dolomite problem: Control of precipitation kinetics by temperature and saturation state. *American Journal of Science*, 299:257–288.

Baniak, G. M., Gingras, M. K., and Pemberton, S. G. 2013. Reservoir characterization of burrow-associated dolomites in the Upper Devonian Wabamun Group, Pine Creek Gas Field, Central Alberta, Canada. *Marine and Petroleum Geology*, 48:275–292.

Bathurst, R. G. C. 1966. Boring algae, micrite envelopes and lithification of molluscan biosparites. *Geological Journal*, 5:15–32.

Beales, F. W. 1953. Dolomitic mottling in Palliser (Devonian) limestone, Banff and Jasper National Parks, Alberta. *American Association of Petroleum Geologists Bulletin*, 37:2281–2293.

Behairy, A. K. A., Durgaprasada Rao, N. V. N., and El-Shater, A. 1991. A siliciclastic coastal sabkha, Red Sea Coast, Saudi Arabia. *Journal of King Abdulaziz University (JKAU) Marine Science*, 2:65–77.

Bromley, R. G. 1996. Trace Fossils: Biology, Taphonomy and Applications, 2nd Edition. Chapman and Hall, London, 361 p.

Bromley, R. G. and Ekdale, A. A. 1984. *Chondrites*: A trace fossil indicator of anoxia in sediments. *Science*, 224:872–874.

Bruckschen, P., Oesmann, S., and Veizer, J. 1999. Isotope stratigraphy of the European Carboniferous: Proxy signatures for ocean chemistry, climate, and tectonics. *Chemical Geology*, 161:127–163.

Budd, D. A. 1997. Cenozoic dolomites of carbonate islands: Their attributes and origin. *Earth-Science Reviews*, 42:1–47.

Butler, G. P. 1969. Modern evaporite deposition and geochemistry of coexisting brines, the sabkha, Trucial Coast, Arabian Gulf. *Journal of Sedimentary Petrology*, 39:70–89.

Canfield, D. E., Thamdrup, B., and Hansen, J. W. 1993. The anaerobic degradation of organic matter in Danish coastal sediments: Iron reduction, manganese reduction, and sulfate reduction. *Geochimica et Cosmochimica Acta*, 57:3867–3883.

Cant, D. J. 1988. Regional structure and development of the Peace River Arch, Alberta: A Paleozoic failed-rift system? *Bulletin of Canadian Petroleum Geology*, 36:284–295.

Chapelle, F. H., Vroblesky, D. A., McMahon, P. B., Dubrovsky, N. M., Fujii, R. F., and Oaksford, E. T. 1995. Deducing the distribution of terminal electron-accepting processes in hydrologically diverse groundwater systems. *Water Resources Research*, 31:359–371.

Choquette, P. W. and Pray, L. C. 1970. Geologic nomenclature and classification of porosity in sedimentary carbonates. *American Association of Petroleum Geologists Bulletin*, 54:207–250.

Cioppa, M. T., Al-Aasm, I. S., Symons, T. A., and Gillen, K. P. 2003. Dating penecontemporaneous dolomitization in carbonate reservoirs: Paleomagnetic, petrographic, and geochemical constraints. *American Association of Petroleum Geologists Bulletin*, 87:71–88.

Compton, J. S. 1988. Degree of supersaturation and precipitation of organogenic dolomite. *Geology*, 16:318–321.

Confer D. R. and Logan, B. E. 1998. Location of protein and polysaccharide hydrolytic activity in suspended and biofilm wastewater cultures. *Water Research*, 32:31–38.

Corlett, H. J. and Jones, B. 2012. Petrographic and geochemical contrasts between calcite- and dolomite-filled burrows in the Middle Devonian Lonely Bay Formation, Northwest Territories, Canada: Implications for dolomite formation in Paleozoic burrows. *Journal of Sedimentary Research*, 82:648–663.

Craig, H. 1957. Isotopic standards for carbon and oxygen and correction factors for mass-spectrometric analysis of carbon dioxide. *Geochimica et Cosmochimica Acta*, 12:133–149.

Davies, G. R. 1970. Algal-laminated sediments, Gladstone Embayment, Shark Bay, Western Australia. *In* Logan, B. W., Davies, G. R., Read, J. F., and Cebulski, D. E. (eds.), Carbonate Sedimentation and Environments, Shark Bay, Western Australia. American Association of Petroleum Geologists Memoir, 13:169–205.

Decho, A. W. 1990. Microbial exopolymer secretions in ocean environments: Their role(s) in food webs and marine processes. *Oceanography and Marine Biology Annual Review*, 28:73–154.

Diedrich, C., Caldwell, M. W., and Gingras, M. 2011. High-resolution stratigraphy and palaeoenvironments of the intertidal flats to lagoons of the Cenomanian (Upper Cretaceous) of Hvar Island, Croatia, on the Adriatic Carbonate Platform. *Carbonates and Evaporites*, 26:381–399.

Dimitrakopoulos, R. and Muehlenbachs, K. 1987. Biodegradation of petroleum as a source of ^{13}C-enriched carbon dioxide in the formation of carbonate cement. *Chemical Geology*, 65:283–291.

Dixon, J. 1976. Patterned carbonate- a diagenetic feature. *Bulletin of Canadian Petroleum Geology*, 24:450–456.

Douglas, R. J. W., Gabrielse, H., Wheeler, J. O., Stott, D. F., and Belyea, H. R. 1970. Geology of western Canada. *In* Douglas, R. J. W. (ed.), Geology and Economic Minerals of Canada. Geological Survey of Canada Economic Geology Report, 1:366–488.

Durocher, S. and Al-Aasm, I. S. 1997. Dolomitization and neomorphism of Mississippian (Visean) upper Debolt Formation, Blueberry field, northeastern British Columbia: Geologic, petrologic, and chemical evidence. *American Association of Petroleum Geologists Bulletin*, 81:954–977.

Ekdale, A. A. 1988. Pitfalls of paleobathymetric interpretations based on trace fossil assemblages. *Palaios*, 3:464–472.

Ekdale, A. A. and Mason, T. R. 1988. Characteristic trace-fossil associations in oxygen-poor sedimentary environments. *Geology*, 16:720–723.

Ekdale, A. A. and Lewis, D. W. 1991. The New Zealand *Zoophycos* revisited: Morphology, ethology, and paleoecology. *Ichnos*, 1:183–194.

Enos, P. 1983. Shelf environment. *In* Scholle, P. A., Bebout, D. G., and Moore, C. H. (eds.), Carbonate Depositional Environments. American Association of Petroleum Geologists Memoir, 33:267–295.

Epstein, S., Graf, D. L., and Degans, D. T. 1964. Oxygen isotope studies on the origin of dolomite. *In* Craig, H., Miller, S. L., and Wasserburg, J. G. (eds.), Isotopic and Cosmic Chemistry. North-Holland Publishing Co., Amsterdam, pp. 169–180.

Evans, G. 1966. The recent sedimentary facies of the Persian Gulf region. *Philosophical Transactions of the Royal Society A*, 259:291–298.

Franks, J. and Stolz, J. F. 2009. Flat laminated microbial mat communities. *Earth Science Reviews*, 96:163–172.

Froelich, P. N., Klinkhammer, G. P., Bender, M. L., Luedtke, N., Heath, G. R., Cullen, D., Dauphin, P., Hammond, D., Hartman, B., and Maynard, V. 1979. Early oxidation of organic matter in pelagic sediments of the eastern equatorial Atlantic; suboxic diagenesis. *Geochimica et Cosmochimica Acta*, 43:1075–1090.

Garrison, R. E. and Luternauer, J. L. 1971. Textures of calcitic cements formed during early diagenesis, Fraser Delta, British Columbia. *In* Bricker, O. P. (ed.), Carbonate Cements. Johns Hopkins Press, Baltimore, MD, pp. 151–154.

Gerdes, G., Klenke, T., and Noffke, N. 2000. Microbial signatures in peritidal siliciclastic sediments: A catalogue. *Sedimentology*, 47:279–308.

Gingras, M. K., Pemberton, S. G., Muelenbachs, K., and Machel, H. 2004. Conceptual models for burrow-related, selective dolomitization with textural and isotopic evidence from the Tyndall Stone, Canada. *Geobiology*, 2:21–30.

Gingras, M. K., Bann, K. L., MacEachern, J. A., Waldron, J., and Pemberton, S. G. 2007a. A conceptual framework for the application of trace fossils. *In* MacEachern, J. A., Bann, K. L., Gingras, M. K., and Pemberton, S. G. (eds.), Applied Ichnology. Society of Economic Paleontologists and Mineralogists, Short Course Notes, 52:1–26.

Gingras, M. K., Pemberton, S. G., Henk, F., MacEachern, J. A., Mendoza, C. A., Rostron, B., O'Hare, R., and Spila, M. V. 2007b. Applications of ichnology to fluid and gas production in hydrocarbon reservoirs. *In* MacEachern, J. A., Bann, K. L., Gingras, M. K., and Pemberton, S. G.

(eds.), Applied Ichnology. Society of Economic Paleontologists and Mineralogists, Short Course Notes, 52:129–143.

Gingras, M. K., Baniak, G., Gordon, J., Hovikoski, J., Konhauser, K. O., La Croix, A., Lemiski, R., Mendoza, C., Pemberton, S. G., Polo, C., and Zonneveld, J. -P. 2012. Porosity and permeability in bioturbated sediments. *In* Knaust, D. and Bromley, R. G. (eds.), Trace Fossils as Indicators of Sedimentary Environments. Developments in Sedimentology, 64, Elsevier, Amsterdam, pp. 837–868.

Gunatilaka, A. 1987. The dolomite problem in the light of the recent studies. *Modern Geology*, 11:311–324.

Gunatilaka, A., Al-Zamel, A., Shearman, D. J., and Reda, A. 1987. A spherulitic fabric in selectively dolomitized siliciclastic crustacean burrows, northern Kuwait. *Journal of Sedimentary Petrology*, 57:922–927.

Gunnarsson, J. S., Granberg, M. E., Nilsson, H.C., Rosenberg, R., and Hellman, B. 1999a. Influence of sediment organic matter quality on growth and polychlorobiphenyl bioavailability in *Echinodermata* (*Amphiura filiformis*). *Environmental Toxicology and Chemistry*, 18:1534–1543.

Gunnarsson, J. S., Hollertz, K., and Rosenberg, R. 1999b. Effects of organic enrichment and burrowing activity of the polychaete Neries diversicolor on the fate of tetrachlorobiphenyl in marine sediments. *Environmental Toxicology and Chemistry*, 18:1149–1156.

Hardie, L. A. 2003. Anhydrite and gypsum. *In* Middleton, G. V. (ed.), Encyclopedia of Sediments and Sedimentary Rocks. Kluwer Academic Publishers, Dordrecht, pp. 16–19.

Hauck, T. E., Dashtgard, S. E., and Gingras, M. K. 2008. Relationships between organic carbon and Pascichnia morphology in intertidal deposits: Bay of Fundy, New Brunswick, Canada. *Palaios*, 23:336–343.

Hein, F. J. 1999. Mixed ("multi") fractal analysis of Granite Wash fields/pools and structural lineaments, Peace River Arch area, northwestern Alberta, Canada: A potential approach for use in hydrocarbon exploration. *Bulletin of Canadian Petroleum Geology*, 47:556–572.

Hsü, K. J. and Siegenthaler, C. 1969. Preliminary experiments on hydrodynamic movement induced by evaporation and their bearing on the dolomite problem. *Sedimentology*, 12:11–25.

James, N. P. and Kendall, A. C. 1992. Introduction to carbonate and evaporite facies models. *In* Walker, R. G. and James, N. P. (eds.), Facies Models and Sea Level Changes. Geological Association of Canada, pp. 265–276.

Kendall, A. C. 1977a. Origin of dolomite mottling in Ordovician limestones from Saskatchewan and Manitoba. *Bulletin of Canadian Petroleum Geology*, 25:450–504.

——— 1977b. Patterned carbonate—a diagenetic feature by James Dixon. Discussion. *Bulletin of Canadian Petroleum Geology*, 25:695–697.

Kendall, A. C. 2010. Marine evaporites. *In* James, N. P. and Dalrymple, R. W. (eds.), Facies Models 4. Geological Association of Canada, pp. 505–539.

Keswani, A. D. 1999. An integrated ichnological perspective for carbonate diagenesis. M.Sc. thesis, University of Alberta, Canada, 124 p.

Kirkham, A. 2004. Patterned dolomites: Microbial origins and clues to vanished evaporites in the Arab Formation, Upper Jurassic, Arabian Gulf. *In* Braithwaite, C. J. R., Rizzi, G., and Darke, G. (eds.), The Geometry and Petrogenesis of Dolomite Hydrocarbon Reservoirs. Geological Society, London, Special Publication, 235:301–308.

Konhauser, K. O. 2007. Introduction to Geomicrobiology. Blackwell Sciences, Oxford, 440 p.

Konhauser, K. O. and Gingras, M. K. 2007. Linking geomicrobiology with ichnology in marine sediments. *Palaios*, 22:339–342.

Konhauser, K. O. and Gingras, M. K. 2011. Are animal burrows a major sedimentary sink for metals? *Ichnos*, 18:144–146.

Krause, S., Liebetrau, V., Gorb, S., Sánchez-Romá, M., McKenzie, J. A., and Treude, T. 2012. Microbial nucleation of Mg-rich dolomite in exopolymeric substances under anoxic modern seawater salinity: New insight into an old enigma. *Geology*, 40:587–590.

Kristensen, E. 2000. Organic matter diagenesis at the oxic/anoxic interface in coastal marine sediments, with emphasis on the role of burrowing animals. *Hydrobiologia*, 426:1–24.

Krumbein, W. C. and Garrels, R. M. 1952. Origin and classification of chemical sediments in terms of pH and oxidation-reduction potentials. *Journal of Geology*, 60:1–33.

Krumbein, W. E. 1994. The year of the slime. *In* Krumbein, W. E., Paterson, D. M., and Stall, L. J. (eds.), Biostabilization of Sediments. University of Oldenburg, Oldenburg, Germany, pp. 1–7.

Krumbein, W. E. and Cohen, Y. 1977. Primary production, mat formation and lithification: contribution of oxygenic and facultative anoxygenic cyanobacteria. *In* Flügel, E. (ed.), Fossil Algae: Resent Results and Development. Springer-Verlag, Berlin, pp. 37–56.

Lalonde, S. V., Dafoe, L., Pemberton, S. G., Gingras, M. K., and Konhauser, K. O. 2010. Investigating the geochemical impact of burrowing animals: Proton and cadmium adsorption onto the mucus-lining of *Terebellid* polychaete worms. *Chemical Geology*, 271:44–51.

Land, L. S. 1980. The isotopic and trace element geochemistry of dolomite: The state of the art. *In* Zenger, D. H., Dunham, J. B., and Ethington, R. L. (eds.), Concepts and Models of Dolomitization. Society of Economic Paleontologists and Mineralogists, Special Publication, 28: 87–110.

Land, L. S. 1998. Failure to precipitate dolomite at 25°C from dilute solutions despite 1000-fold oversaturation after 32 years. *Aquatic Geochemistry*, 4:361–368.

Land, L. S. and Moore, C. H. 1980. Lithification, micritization and syndepositional diagenesis of biolithies on the Jamaican Island slope. *Journal of Sedimentary Petrology*, 50:357–370.

Law, J. 1981. Mississippian correlations, northeastern British Columbia, and implications for oil and gas exploration. *Bulletin of Canadian Petroleum Geology*, 29:378–398.

Logan, B. W. 1961. Cryptozoon and associate stromatolites from the recent, Shark Bay, Western Australia. *Journal of Geology*, 69:517–533.

Macauley, G. 1958. Late Paleozoic of Peace River area. *In* Woodman, A. J. (ed.), Jurassic and Carboniferous of Western Canada. American Association of Petroleum Geologists, John Andrew Allan Memorial Volume, pp. 289–308.

MacEachern, J. A., Pemberton, S. G., Bann, K. L., and Gingras, M. K. 2007. Departures from the archetypal ichnofacies: Effective recognition of environmental stress in the rock record. *In* MacEachern, J. A., Bann, K. L., Gingras, M. K., and Pemberton, S. G. (eds.), Applied Ichnology. Society of Economic Paleontologists and Mineralogists, Short Course Notes, 52:65–92.

Machel, H. G. 1993. Anhydrite nodules formed during deep burial. *Journal of Sedimentary Petrology*, 63:659–662.

Machel, H. G. 2004. Concepts and models of dolomitization: A critical appraisal. *In* Braithwaite, C. J. R., Rizzi, G., and Darke, G. (eds.), The Geometry and Petrogenesis of Dolomite Hydrocarbon Reservoirs. Geological Society, London, Special Publication, 235:7–63.

Machel, H. G. and Mountjoy, E. W. 1986. Chemistry and environments of dolomitization—a reappraisal. *Earth Science Reviews*, 23:175–222.

Machel, H. G. and Burton, E. A. 1991. Burial-diagenetic sabkha-like gypsum and anhydrite nodules. *Journal of Sedimentary Petrology*, 61:394–405.

Markham, G. D., Glusker, J. P., and Bock, C. W. 2002. The arrangement of first- and second-sphere water molecules in divalent magnesium complexes: Results from molecular orbital and density functional theory and from structural crystallography. *The Journal of Physical Chemistry B*, 106:5118–5134.

Mayer, C., Moritz, R., Kirschner, C., Borchard, W., Maibaum, R., Wingender, J., and Flemming, H.-C. 1999. The role of intermolecular interactions: Studies on model systems for bacterial biofilms. *International Journal of Biological Macromolecules*, 26:3–16.

Mazzullo, S. J. 2000. Organogenic dolomitization in peritidal to deep-sea sediments. *Journal of Sedimentary Research*, 70:10–23.

McCrea, J. M. 1950. On the isotopic chemistry of carbonates and a paleotemperature scale. *The Journal of Chemical Physics*, 18:849–857.

McKenzie, J. A. 1981. Holocene dolomitization of calcium-carbonate sediments from the coastal sabkhas of Abu Dhabi, U.A.E.: A stable isotope study. *Journal of Geology*, 89:185–198.

McKenzie, J. A. 1991. The dolomite problem: An outstanding controversy. *In* Müller, D. W., McKenzie, J. A., and Weissert, H. (eds.), Controversies in Modern Geology: Evolution of Geological Theories in Sedimentology, Earth history, and Tectonics. Academic Press, London, pp. 37–54.

Miller, M. F. 1991. Morphology and paleoenvironmental distribution of Paleozoic *Spirophyton* and *Zoophycos*: Implications for the *Zoophycos* ichnofacies. *Palaios*, 6:410–425.

Morrow, D. W. 1978. Dolomitization of Lower Paleozoic burrow fillings. *Journal of Sedimentary Petrology*, 48:295–306.

Morrow, D. W. 1982. Diagenesis 1: Dolomite-part 1, the chemistry of dolomitization and dolomite precipitation. *Geoscience Canada*, 9:5–13.

Needham, S. J., Worden, R. H., and McIlory, D. 2004. Animal sediment interactions: The effect of ingestion and excretion by worms on mineralogy. *Biogeosciences*, 1:113–121.

Nicholson, J. A. M., Stolz, J. F., and Pierson, B. K. 1987. Structure of a microbial mat in a saltmarsh. *Federation of European Microbiological Societies (FEMS) Microbiology Ecology*, 45:343–364.

Northrop, D. A. and Clayton, R. N. 1966. Oxygen-isotope fractionations in systems containing dolomite. *Journal of Geology*, 74:174–196.

O'Connell, S. C., Dix, G. R., and Barclay, J. E. 1990. The origin, history, and regional structural development of the Peace River Arch, Western Canada. *Bulletin of Canadian Petroleum Geology*, 38A:4–24.

O'Connell, S. C. 1994. Geological history of the Peace River Arch. *In* Mossop, G. D. and Shetsen, I. (comps.), Geological Atlas of the Western Canada Sedimentary Basin. Canadian Society of Petroleum Geologists and Alberta Research Council, pp. 431–438.

O'Neil, J. R. and Epstein, S. 1966. Oxygen isotope fractionation in the system dolomite-calcite-carbon dioxide. *Science*, 152:198–201.

Packard, J. J., Al-Aasm, I. S., and Devon Canada Exploration Team. 2004. Reflux dolomitization of Mississippian-age sabkha and restricted subtidal sediments resulting in a 1.6 Tcf giant gas field: The Upper Debolt Formation of west-central Alberta. Canadian Society of Petroleum Geologists, Core Seminar and Abstracts, Calgary, Alberta, 26 p.

Pak, R., Pemberton, S. G., and Stasiuk, L. 2010. Paleoenvironmental and taphonomic implications of trace fossils in Ordovician kukersites. *Bulletin of Canadian Petroleum Geology*, 58:141–158.

Petrash, D. A., Lalonde, S. V., Gingras, M. K., and Konhauser, K. O. 2011. A surrogate approach to studying the chemical reactivity of burrow mucous linings in marine sediments. *Palaios*, 26:595–602.

Qing, H. and Nimegeers, A. R. 2008. Lithofacies and depositional history of Midale carbonate-evaporite cycles in a Mississippian ramp setting, Steelman-Bienfait area, southeastern Saskatchewan, Canada. *Bulletin of Canadian Petroleum Geology*, 56:209–234.

Rameil, N. 2008. Early diagenetic dolomitization and dedolomitization of Late Jurassic and earliest Cretaceous platform carbonates: A case study from the Jura Mountains (NW Switzerland, E France). *Sedimentary Geology*, 212:70–85.

Reeburgh, W. S. 1980. Anaerobic methane oxidation: Rate depth distributions in Skan Bay sediments. *Earth and Planetary Science Letters*, 47:345–352.

Reitsema, R. H. 1980. Dolomite and nahcolite formation in organic rich sediments: Isotopically heavy carbonates. *Geochimica et Cosmochimica Acta*, 44:2045–2049.

Richards, B. C. 1989. Upper Kaskaskia sequence: Uppermost Devonian and Lower Carboniferous. *In* Ricketts, B. D. (ed.), *Western Canada Sedimentary Basin: A Case History*. Canadian Society of Petroleum Geologists, 165–201.

Richards, B. C., Bamber, E. W., Higgins, A. C., and Utting, J. 1993. Carboniferous. *In* Stott, D. F. and Aitken, J. D. (eds.), Sedimentary Cover of the Craton in Canada. Geological Survey of Canada, Geology of Canada, 5:202–271.

Richards, B. C., Barclay, J. E., Bryan, D., Hartling, A., Henderson, C. M., and Hinds, R. C. 1994. Carboniferous strata of the western Canada sedimentary basin. *In* Mossop, G. D. and Shetsen, I. (comps.), Geological Atlas of the Western Canada Sedimentary Basin. Canadian Society of Petroleum Geologists and Alberta Research Council, pp. 221–249.

Roberts, J. A., Bennett, P. C., Gonzales, L. A., Macpherson, G. L., and Milliken, K. L. 2004. Microbial precipitation of dolomite in methanogenic groundwater. *Geology*, 32:277–280.

Sibley, D. F. and Gregg, J. M. 1987. Classification of dolomite rock textures. *Journal of Sedimentary Petrology*, 57:967–975.

Steward C. C., Nold, S. C., Ringelberg, D. B., White, D. C., and Lovell, C. R. 1996. Microbial biomass and community structures in the burrows of bromophenol producing and non-producing marine worms and surrounding sediments. *Marine Ecology Progress Series*, 133: 149–165.

Stolz, J. F. 1990. Distribution of phototrophic microbes in the flat laminated microbial mat at Laguna Figueroa, Baja California, Mexico. *Biosystems*, 23:345–357.

Taylor, M. E. and Halley, R. B. 1974. Systematics, environments, and biogeography of some Late Cambrian and Early Ordovician trilobites from eastern New York State. United States Geological Survey Professional Paper 834, 38 p.

Thompson, L. C. and Pritchard, A. C. 1969. Osmoregulatory capacities of *Callianassa* and *Upogebia* (Crustacea: Thalassinidea). *Biological Bulletin*, 136:114–129.

Van Lith, Y., Warthmann, R., Vasconcelos, C., and McKenzie, J. A. 2003. Sulfate-reducing bacteria induce low-temperature Ca-dolomite and high Mg-calcite formation. *Geobiology*, 1:71–79.

Vasconcelos, C. and McKenzie, J. A. 1997. Microbial mediation of modern dolomite precipitation and diagenesis under anoxic conditions (Lagoa Vermelha, Rio de Janeiro, Brazil). *Journal of Sedimentary Research*, 67:378–390.

Vasconcelos, C., McKenzie, J. A., Bernasconi, S., Grujic, D., and Tien, A. J. 1995. Microbial mediation as a possible mechanism for natural dolomite formation at low temperatures. *Nature*, 377:220–222.

Vasconcelos, C., McKenzie, J. A., Warthmann, R., and Bernasconi, S. M. 2005. Calibration of the $\delta^{18}O$ paleothermometer for dolomite precipitated in microbial cultures and natural environments. *Geology*, 33:317–320.

Von der Borch, C. C. and Lock, D. 1979. Geological significance of Coorong dolomites. *Sedimentology*, 26:813–824.

Wacey, D., Wright, D. T., and Boyce, A. J. 2007. A stable isotope study of microbial dolomite formation in the Coorong Region, South Australia. *Chemical Geology*, 244:155–174.

Warren, J. K. 2000. Dolomite: Occurrence, evolution and economically important associations. *Earth-Science Reviews*, 52:1–81.

Warren, J. K. and Kendall, C. G. S. 1985. Comparison of sequences formed in marine sabkha (subaerial) and salina (subaqueous) settings- modern and ancient. *American Association of Petroleum Geologists Bulletin*, 89:1013–1023.

Warthmann, R., Lith, Y. V., Vasconcelos, C., McKenzie, J. A., and Karpoff, A. M. 2000. Bacterially induced dolomite precipitation in anoxic culture experiments. *Geology*, 28:1091–1094.

Warthmann, R., Vasconcelos, C., Sass, H., and McKenzie, J. A. 2005. *Desulfovibrio brasiliensis* sp. nov., a moderate halophilic sulfate-reducing bacterium from Lagoa Vermelha (Brazil) mediating dolomite formation. *Extremephiles*, 9:255–261.

Waslenchuk, D. G., Matson, E. A., Zajac, R. N., Dobbs, F. C., and Tramontano, J. M. 1983. Geochemistry of burrow waters vented by a bioturbating shrimp in Bermudian sediments. *Marine Biology*, 72:219–225.

Wright, D. T. and Wacey, D. 2005. Precipitation of dolomite using sulfate-reducing bacteria from the Coorong Region, South Australia: Significance and implication. *Sedimentology*, 52:987–1008.

Zenger, D. H. 1996. Dolomitization patterns in widespread 'Bighorn Facies' (Upper Ordovician), Western Craton, USA. *Carbonates and Evaporites*, 11:219–225.